МІНІСТЕРСТВО ОСВІТИ І НАУКИ УКРАЇНИ
НАЦІОНАЛЬНИЙ АВІАЦІЙНИЙ УНІВЕРСИТЕТ
ФАКУЛЬТЕТ АЕРОНАВІГАЦІЇ, ЕЛЕКТРОНІКИ ТА ТЕЛЕКОМУНІКАЦІЙ
КАФЕДРА АЕРОКОСМІЧНИХ СИСТЕМ УПРАВЛІННЯ

ДОПУСТИТИ ДО ЗАХИСТУ
Завідувач кафедри
_____Юрій МЕЛЬНИК
«_____» _____2024 р.

КВАЛІФІКАЦІЙНА РОБОТА

(ПОЯСНЮВАЛЬНА ЗАПИСКА)

ВИПУСКНИКА ОСВІТНЬОГО СТУПЕНЯ
«БАКАЛАВР»

Тема: «**Визначення та аналіз складових дрейфу зміщення нуля мікроелектромеханічних акселерометрів з використанням дисперсії Аллана**»

Виконавець: студент групи СУ-404 _____ Вадим ЖЕРЕВЧУК

Керівник: професор _____ Валерій ЧІКОВАНІ

Нормоконтролер: _____ Микола ДИВНИЧ

Київ 2024

MINISTRY OF EDUCATION AND SCIENCE OF UKRAINE
NATIONAL AVIATION UNIVERSITY
FACULTY OF AIR NAVIGATION, ELECTRONICS AND TELECOMMUNICATIONS
AEROSPACE CONTROL SYSTEMS DEPARTMENT

APPROVED FOR DEFENCE
Head of the Department
_____ Yurii MELNYK
"____" _____ 2024

QUALIFICATION PAPER

(EXPLANATORY NOTE)

FOR THE ACADEMIC DEGREE OF BACHELOR

Title: **"The determination and analysis of microelectromechanical accelerometer bias drift components using the Allan variance**"

Submitted by: student of group CS-404 _____ Vadym ZHEREVCHUK

Supervisor: professor _____ Valerii CHIKOVANI

Standards inspector: _____ Mykola DYVNYCH

Kyiv 2024

НАЦІОНАЛЬНИЙ АВІАЦІЙНИЙ УНІВЕРСИТЕТ

Факультет аеронавігації, електроніки та телекомунікацій

Кафедра аерокосмічних систем управління

Спеціальність: 151 «Автоматизація та комп'ютерно-інтегровані технології»

ЗАТВЕРДЖУЮ

Завідувач кафедри

_____ Юрій МЕЛЬНИК

«_____»_____2024 р.

ЗАВДАННЯ

на виконання кваліфікаційної роботи

Жеревчука Вадима Васильовича

1. Тема кваліфікаційної роботи «Визначення та аналіз складових дрейфу зміщення нуля мікроелектромеханічних акселерометрів з використанням дисперсії Аллана» затверджена наказом ректора від «01» квітня 2024 р. № 511/ст.

2. Термін виконання роботи: з 13.05.2024 по 16.06.2024.

3. Вихідні дані роботи: Експериментальні дані багатогодинних випробувань акселерометра з кварцовим чутливим елементом Французького виробництва та MMA8451Q MEMC акселерометра компанії NXP (США).

4. Зміст пояснювальної записки: Вступ, розділ 1 - мікроелектромеханічні акселерометри, розділ 2 – варіація Аллана та опис випадкових похибок, розділ 3 – Застосування методу варіації Аллана до високоточного кварцового акселерометра, висновки, література.

5. Перелік обов’язкового ілюстративного матеріалу: Графіки результатів випробувань та графічне представлення кривих Аллана. Матеріали презентації в Power Point.

6. Календарний план-графік

№ пор.	Завдання	Термін виконання	Відмітка про виконання
1	Отримання теми дипломної роботи	13.05.2024	Виконано
2	Написання першого розділу роботи	17.05.2024	Виконано
3	Написання другого розділу роботи	27.05.2024	Виконано
4	Подача керівнику першого та другого розділів на перевірку	28.05.2024	Виконано
5	Написання третього розділу роботи	7.06.2024	Виконано
6	Подача керівнику третього розділу на перевірку	8.06.2024	Виконано
7	Оформлення дипломної роботи	12.06.2024	Виконано
8	Підготовка презентації доповіді	16.06.2024	Виконано

7. Дата видачі завдання: «13» травня 2024 р.

Керівник кваліфікаційної роботи _____ Валерій ЧІКОВАНІ
(підпис керівника)

Завдання прийняв до виконання _____ Вадим ЖЕРЕВЧУК
(підпис випускника)

NATIONAL AVIATION UNIVERSITY

Faculty of Air Navigation, Electronics and Telecommunications

Aerospace Control Systems Department

Specialty: 151 “Automation and Computer-integrated Technologies”

APPROVED BY

Head of the Department

_____ Yurii MELNYK

“_____”_____2024

Qualification Paper Assignment for Graduate Student

Vadym Zherevchuk Vasylovych

1. The qualification paper title “The determination and analysis of microelectromechanical accelerometer bias drift components using the Allan variance” was approved by the Rector’s order of “ 01 ” April 2024 № 511/ст.

2. The paper to be completed between: 13.05.2024 and 16.06.2024

3. Initial data for the paper: Experimental data of many hours of tests of the accelerometer with a quartz sensitive element of French production and the MMA8451Q MEMS accelerometer of the company NXP (USA).

4. The content of the explanatory note: Introduction, section 1 - microelectromechanical accelerometers, section 2 - the Allan variance and random errors description, section 3 - application of the allan variance method to high accurate quartz accelerometer, conclusion, references.

5. The list of mandatory illustrations: Graphs of test results and graphical presentation of Allan curves. Presentation materials in Power Point

6. Timetable

№	Assignment	Dates of completion	Completion mark
1	Obtaining a thesis topic	13.05.2024	Done
2	Writing the first chapter of the work	17.05.2024	Done
3	Writing the second chapter of the work	27.05.2024	Done
4	Submitting the first and second sections to the manager for review	28.05.2024	Done
5	Writing the third chapter of the work	7.06.2024	Done
6	Submission to the head of the third section for review	8.06.2024	Done
7	Completion of the thesis	12.06.2024	Done
8	Preparation of the presentation of the report	16.06.2024	Done

7. Assignment issue date: “13” May 2024

Qualification paper supervisor _____ Valerii CHIKOVANI
(the supervisor’s signature)

Issued task accepted _____ Vadym ZHEREVCHUK
(the graduate student’s signature)

РЕФЕРАТ

Пояснювальна записка до дипломної роботи "Визначення та аналіз складових дрейфу зміщення нуля мікроелектромеханічних акселерометрів з використанням дисперсії Аллана" містить 70 сторінок, 35 ілюстрацій, 38 джерел.

Актуальність теми полягає в необхідності точного визначення складових шуму сучасних високоякісних акселерометрів для визначення їхньої точності та напрямків їх застосування, таких як навігаційні системи, космічні та авіаційні технології, а також побудування моделей похибок для їх корегування.

Об'єктом дослідження є акселерометр навігаційного класу точності в що входить у склад інерціального вимірювальному блоку.

Предметом дослідження є метод варіації Аллана для високоякісного акселерометра з кварцовим чутливим елементом.

Метою роботи є вивчання методів аналізу та моделювання випадкових похибок акселерометрів з використанням методу варіації Аллана для визначення напрямків їх застосування та побудування моделей похибок з метою їх корегування для підвищення точності.

Методи дослідження Розробка комп’ютерних програм для розрахунків параметрів компонентів шуму, графічне визначення параметрів компонентів випадкових похибок, аналітичний аналіз методу варіації Аллана.

Ключові слова: МІКРОЕЛЕКТРОМЕХАНІЧНІ СИСТЕМИ (МЕМС), АКСЕЛЕРОМЕТРИ, ІНЕРЦІАЛЬНИЙ ВИМІРЮВАЛЬНИЙ БЛОК, АЛГОРИТМИ, МЕТОД ВАРІАЦІЇ АЛЛАНА.

ABSTRACT

Explanatory note for the qualification paper "The determination and analysis of microelectromechanical accelerometer bias drift components using the Allan variance" includes: 70 pages, 35 illustrations, 38 sources.

Relevance of the topic is the need to accurately determine the noise components of modern high-quality accelerometers to determine their accuracy and areas of application, such as navigation systems, space and aviation technologies, and to build error models for their correction.

The object of the study is an accelerometer of the navigation class of accuracy, which is part of the inertial measuring unit.

The subject of the research is the Allan variation method for a high-quality accelerometer with a quartz sensitive element.

The aim of the work is study methods for analyzing and modeling random errors in accelerometers using the Allan variance method to determine their application area and build error models for increased accuracy.

Research methods are the development of computer programs for parameter calculations, graphical determination of error components, and analytical analysis of the Allan variation method.

Key words: MICROELECTROMECHANICAL SYSTEMS (MEMS), ACCELEROMETERS, INERTIAL MEASUREMENT UNITS, ALGORITHMS, AND THE ALLAN VARIATION METHOD.

CONTENT

INTRODUCTION

High performance capacitive MEMS accelerometers are increasingly being used in various motion sensing applications including medical, industrial, and military requiring measurement of acceleration, vibration, shock, tilt, rotation etc. In a wide range of inertial navigation applications, tactical grade MEMS accelerometers are already the preferred solution due to their small size, low power consumption, and convenient price; however, in Inertial Measurement Units (IMU) and Inertial Navigation Systems (INS), which are designed for navigation grade applications, conventional non-MEMS accelerometers are generally used, such as electromechanical servo and bulk piezoelectric accelerometers. During the past decade, design and initial measurement results of closed-loop MEMS accelerometers were presented, showing the potential of the MEMS technology to deliver a smaller and cheaper sensor while realizing inertial navigation grade performance.

In order to achieve navigation grade performance, high linearity (<0.1%) is an important parameter to satisfy. Linearity may be limited by the capacitive nature of MEMS sensors in which output is inversely proportional to the gap change in the sense capacitor. Closed-loop MEMS accelerometers, which use electrostatic force feedback, balance the sensor structure around its nominal position, neutralizing the influence of the sense capacitor nonlinearity. There is a variety of system design challenges towards attaining navigation-grade level. Firstly, a linear and stable feedback pass must be established. In addition to the improved linearity, other parameters such as short- and long-term bias, scale factor stability, and vibration rectification error (VRE) need to be addressed from the design level in order to satisfy all the requirements during the integration of the sensor system.

SECTION 1

MICROELECTROMECHANICAL ACCELEROMETERS

In today's technological world, microelectromechanical accelerometers (MEMS accelerometers) occupy a special place among sensors, playing an important role in many areas of science and technology. Their applications range from consumer electronics devices to industrial systems, from medical equipment to autonomous vehicles.

MEMS accelerometers can measure acceleration with high accuracy and speed, making them indispensable for many applications where measurement accuracy and device miniaturization are important.

This paper is devoted to an overview of the types of MEMS accelerometers, including pendulum and vibration accelerometers, their operating principles and practical applications. By exploring their structure, functioning and capabilities, we will gain a deeper understanding of these important devices and their role in the current technological paradigm.

This paper will present an analysis of current achievements in the field of MEMS accelerometers, their advantages, disadvantages and prospects for further development. Specific examples of MEMS accelerometers in various fields will also be considered, which will allow to present a wide range of possibilities of these devices.

1.1. Definition of accelerometers

An accelerometer serves as a sensor detecting specific force or changes in velocity over time. When vibrations or shifts in motion occur, the sensor records the force exerted, typically by compressing a piezoelectric material, which generates an electric charge proportional to the force experienced. As charge aligns with force, and mass remains constant, the charge also correlates directly with acceleration. Acceleration is commonly quantified in meters per second squared (m/s^2) or in terms of g-forces (g), with one g-force on Earth approximately equaling 9.8 m/s^2, though this value varies slightly with altitude and differs on other celestial bodies due to gravitational differences.

Accelerometers find utility in various scenarios, including vibration analysis in systems and determining orientation. Their applications span from space stations to handheld gadgets [1].

The principle of operation

An accelerometer can be thought of as a test mass attached to a spring (see in Fig.1.1.1). The displacement is measured to estimate the acceleration. [2].

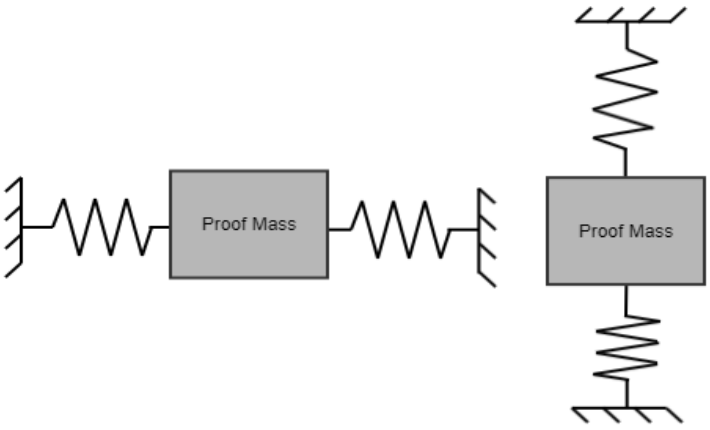

Fig. 1.1.1. The principle of accelerometer operation

Accelerometers possess the capability to measure acceleration along one, two, or three axes. The increasing popularity of 3-axis devices is attributed to diminishing

development costs. Typically, accelerometers integrate capacitive plates, some stationary while others tethered to tiny springs internally, responding to acceleration forces. Movement of these plates relative to each other causes fluctuations in capacitance, serving as a gauge for acceleration determination.

Moreover, certain accelerometers leverage piezoelectric materials as their base. These minuscule crystalline structures produce an electric charge under mechanical stress, including acceleration [3][4].

Main applications of accelerometers

Accelerometers play a crucial role in various sectors including industrial, manufacturing, commercial, and laboratory applications. Here are some examples of their diverse applications:

- Digital devices: Accelerometers integrated into smartphones, digital cameras, and other mobile devices enable automatic screen rotation based on the device's orientation.
- Vehicles: Accelerometers are instrumental in vehicle safety systems, particularly airbags, where they trigger the deployment of airbags upon sensing a sudden impact, thus contributing significantly to saving lives.
- Drones: Accelerometers aid drones in stabilizing their orientation during flight, ensuring smooth and controlled movement.
- Rotating equipment: Accelerometers are utilized in rotating machinery to detect undulating vibrations, helping in identifying potential issues and ensuring optimal performance.
- Industrial platforms: Industrial accelerometers are employed to measure the stability or tilt of platforms in industrial settings, which is crucial for maintaining safety and operational efficiency.
- Vibration monitoring: Accelerometers are valuable for monitoring vibrations generated by moving machinery. Detecting and analyzing these vibrations are

essential for preventing equipment damage and optimizing maintenance schedules. They are increasingly adopted in facilities such as industrial plants and turbines for vibration monitoring and analysis [5].

1.2. Micro-electromechanical systems (MEMS)

MEMS (microelectromechanical systems) technology involves microscopic devices integrating electronic and movable parts. These systems consist of components sized from 1 to 100 micrometers (0.001 to 0.1 mm), while actual MEMS devices typically range from 20 micrometers to a millimeter (0.02 to 1.0 mm) in size. Notably, components organized in arrays, like digital micro-mirror devices, may exceed an area of 1000 mm^2 [6].

Primarily, MEMS technology encompasses miniature mechanical and electromechanical elements, including devices and structures, manufactured using micro-manufacturing techniques. These systems incorporate various components (see Fig. 1.2.1) such as microsensors, microprocessors, microactuators, data processing units, and elements capable of interfacing with external components. Integrating these components at the microscale empowers MEMS devices to execute diverse functions across an extensive array of applications.

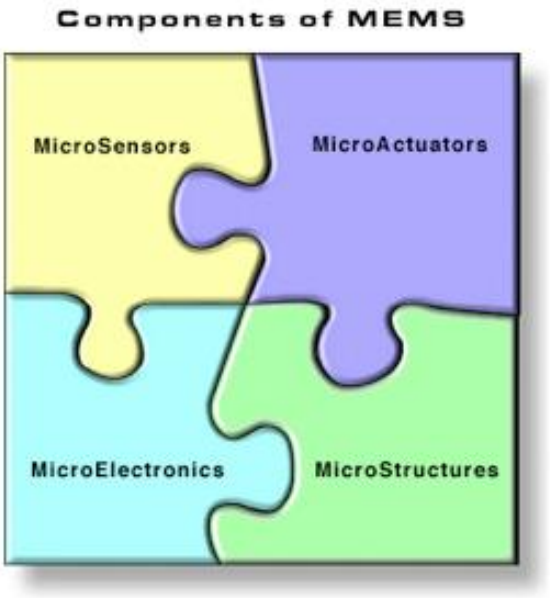

Fig. 1.2.1. Components of MEMS

The critical dimensions of MEMS devices can vary from below one micron to several millimeters. Consequently, the diversity of MEMS devices ranges from simple structures without moving parts to complex electromechanical systems with multiple moving parts controlled by integrated microelectronics.

The defining feature of MEMS is the inclusion of mechanical functionality in at least some elements, regardless of their ability to move. The terminology used to describe MEMS may differ across regions. In the United States, they are primarily known as MEMS, while terms like "microsystems technology" or "micromechanical devices" may be preferred elsewhere.

Key components integral to MEMS include microsensors and microactuators, both classified as "transducers," which convert energy from one form to another. Microsensors typically convert mechanical signals into electrical ones.

Designing MEMS technology poses unique challenges due to its large surface area to volume ratio. This characteristic amplifies the impact of ambient electromagnetism forces, such as electrostatic charges and magnetic moments, and hydrodynamics effects like surface tension and viscosity, compared to larger mechanical devices. It's important to distinguish MEMS technology from molecular nanotechnology or molecular electronics, which also consider surface chemistry in their design and operation.

Principle of MEMS-accelerometer operation

MEMS accelerometers, also known as microelectromechanical system accelerometers, are small, highly accurate sensors used to measure angular velocity and orientation. A MEMS accelerometer works on the principle of angular momentum. Angular momentum is a measure of an object's rotational motion and is defined as the product of the object's mass, velocity, and radius. When an object rotates, it has angular momentum, and the amount of angular momentum depends on the object's mass, velocity, and radius.

A MEMS accelerometer consists of a small microscopic device that is suspended from a flexible structure. This device, called a "test mass," can move freely in any direction. When the test specimen is subjected to an angular acceleration, a force proportional to the angular acceleration and the mass of the test specimen is applied to the test mass. This force causes the test mass to move, and the movement of the test mass is detected by sensors that measure the displacement of the test mass.

Capacitive MEMS technology

In typical MEMS accelerometers, a capacitive design is employed (refer to Fig. 1.2.2), where a mobile comb is linked to a fixed comb via a spring. When there's no acceleration, the mobile comb remains centered, resulting in uniform capacitance across all capacitors. However, when acceleration is applied along the sensing axis, the mobile comb moves, leading to varying capacitance levels on each side of the comb. This disparity in capacitance is directly proportional to the acceleration.

To translate this variance in capacitance into acceleration measurements in standard units, an array of analog components and analog-to-digital converters is utilized. These components collaborate to precisely convert the capacitance variances into meaningful acceleration readings [9].

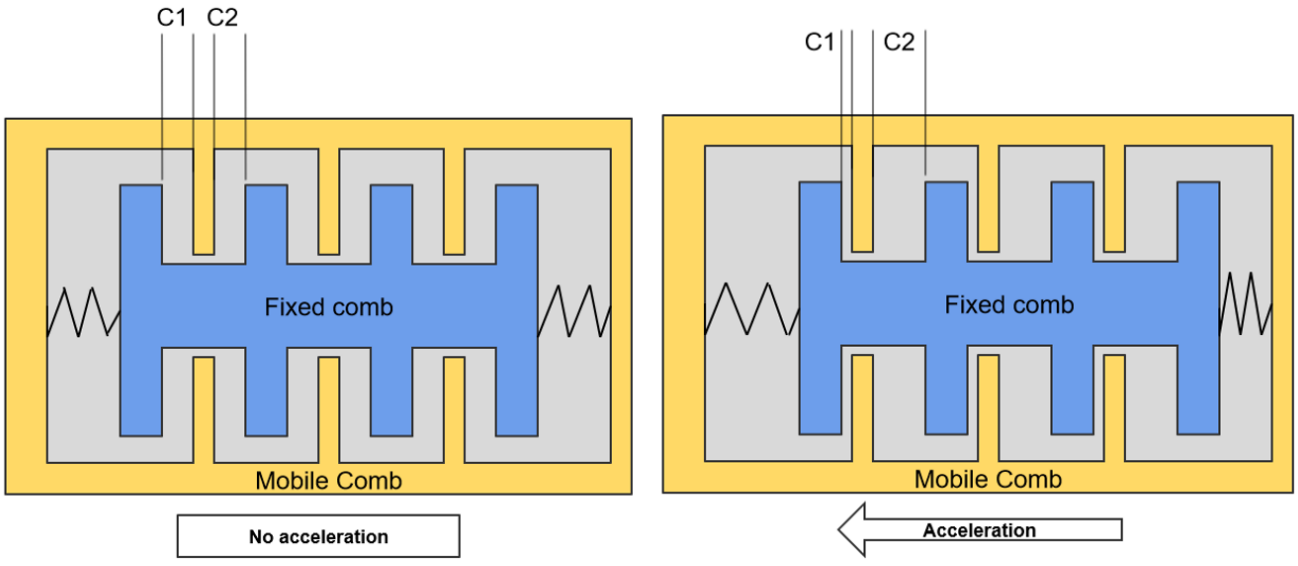

Fig. 1.2.2. Capacitive design

1.3. Introduction to Pendulum MEMS accelerometer

A pendulum accelerometer functions by harnessing the principles of a pendulum's oscillating movement to measure linear acceleration. Its core idea centers on the reactive oscillations of a pendulum induced by external acceleration. By assessing the pendulum's displacement or positional changes, one can infer information about the magnitude and direction of the applied acceleration.

The principle of operation

The mechanism of a pendulum accelerometer (Fig. 1.3.1) rentals a mass suspended from either a rigid or flexible support structure, often a beam or rod. This suspended mass has the freedom to swing around a designated pivot point. When subjected to acceleration, a force acts upon the pendulum, causing it to deviate from its equilibrium position. This deviation or displacement of the pendulum correlates directly with the magnitude of the applied acceleration.

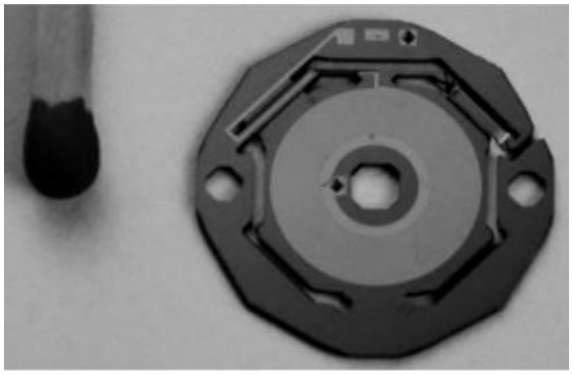

Fig. 1.3.1 Accelerometer pendulum unit

The pendulum accelerometer's fundamental component is its sensing element, which comprises a mass attached to the support frame (base) through suspension elements. These suspension elements can adopt either a cantilever or bridge scheme, each with its specific characteristics.

In the bridge suspension scheme, the mass moves solely along the measuring axis, providing a straightforward measurement setup. On the other hand, the cantilever mass suspension scheme offers high sensitivity but is susceptible to disturbances in the alignment of the frame and mass during significant movements.

Most pendulum micromechanical accelerometers employ a cantilever suspension scheme for their sensing elements. In this scheme, elastic elements resembling beams function in bending or torsion, contributing to the accelerometer's sensitivity and precision.

The design of a pendulum accelerometer, as depicted in Fig. 1.3.2, is tailored to serve as a robust sensing element suitable for various classes and applications within inertial aircraft systems.

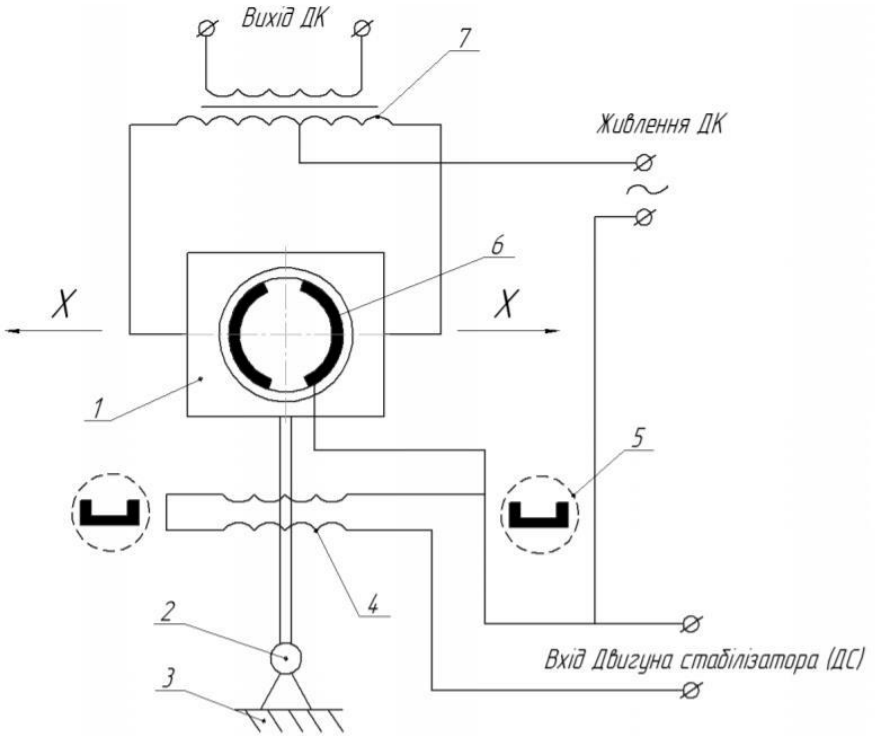

Fig. 1.3.2. Functional diagram of the pendulum accelerometer

The sensing component of the device consists of a physical pendulum (pos.1) suspended elastically (pos.2) with one degree of freedom. When subjected to the Earth's gravitational component along the X-X measuring axis, the pendulum deflects concerning the housing. This deflection is converted into an electrical signal using a

capacitive angle sensor composed of a differential capacitor (item 6) and a differential transformer (item 7), where the AC voltage and phase are determined by the pendulum's deflection direction. The signal from the angle sensor, specifically from the output winding of the differential transformer (item 7), is routed to an amplifier-converter, tasked with amplifying and converting the signal. The amplified signal is then directed to the windings of the magnetoelectric force sensor (pos. 4,5). The resulting moment from the interaction between the current flowing in the force sensor windings and the permanent magnet's field (pos. 5) balances the Earth's gravity component. Thus, the current's magnitude is proportional to the pendulum arm's deviation angle from the vertical. The accelerometer's sensitivity threshold denotes the minimum acceleration it can detect.

The kinematic diagram of the pendulum accelerometer, as depicted in Fig. 1, outlines the configuration of its sensing element, comprising a flat pendulum formed by an inertial mass (m). The pendulum's center of mass is offset from the rotation axis by a distance (l). Two horizontal springs with stiffness (c/2) constrain the pendulum's rotation angles (ϕ) relative to the Ox axis, intersecting at point O perpendicular to the drawing plane [10].

The primary role of the pendulum accelerometer is to measure the acceleration projection onto its measuring axis, aligned with the perpendicular to the pendulum arm in the neutral position of the element's center (axis Ou in Fig. 1.3.3).

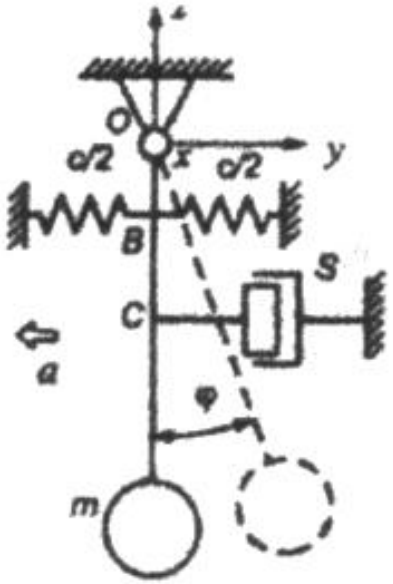

Fig. 1.3.3. Pendulum accelerometer

A notable drawback of pendulum suspensions is their sensitivity to acceleration components along the Oz axis, perpendicular to the sensitivity axis Ou, when the mass deviates from its equilibrium position. This sensitivity increases with the angle ϕ. To mitigate this issue, accelerometers employing such suspensions are often paired with force compensation mechanisms.

Advantages and disadvantages of pendulum accelerometers

Advantages:

- **Simple design:** Pendulum accelerometers have a straightforward design with few components, making them relatively easy to manufacture and maintain.
- **High sensitivity:** Certain types of pendulum accelerometers, such as torsion and inverted pendulums, exhibit high sensitivity to acceleration, making them suitable for precise measurements.
- **Wide range of applications:** Due to their versatility, pendulum accelerometers find use in various applications, from educational purposes to high-precision scientific experiments.

Disadvantages:

- **Size and weight:** Pendulum accelerometers are typically larger and heavier than other types of accelerometers, limiting their suitability for compact or portable applications.
- **Sensitivity to external factors:** Pendulum accelerometers can be sensitive to changes in temperature, airflow, and other environmental factors, affecting their accuracy.
- **Limited bandwidth:** Pendulum accelerometers have a restricted frequency response, making them less suitable for high-frequency or dynamic applications.

Despite their limitations, pendulum accelerometers remain valuable tools in many industries. While they may not excel in compactness or high-frequency applications, their simplicity, sensitivity, and broad applicability make them essential for various engineering and scientific endeavors. Understanding the principles of pendulum accelerometers enables engineers and scientists to optimize their designs, enhance performance, and explore new applications [11].

In terms of latest trends, manufacturers are focusing on developing miniature and high-performance accelerometers to cater to the demand for compact and lightweight applications. The integration of advanced micro-electromechanical systems (MEMS) technology in these accelerometers is also a key trend in the market.

Today, MEMS sensors are rapidly evolving in the scientific and technical domains, emerging as promising devices within modern microsystems technology (MST). The advancement of MEMS sensors and actuators has catalyzed a revolutionary shift in contemporary inertial technology. Leading manufacturers of MEMS accelerometers include Inertial Labs, ENDAQ, Analog Devices Inc. (ADI), CEC Vibration Products, CELIANS, CEMB, AMOT, BeanAir GmbH, CESVA, and CME Technology Co., Ltd [12].

1.4. Inertial Measurement Unit (IMUs) based on pendulum MEMS accelerometers

Tables 1.4.1 and 1.4.2 show the IMUs and the momentary characteristics for each unit [13].

Table 1.4.1

IMUs based on three pendulum accelerometers

	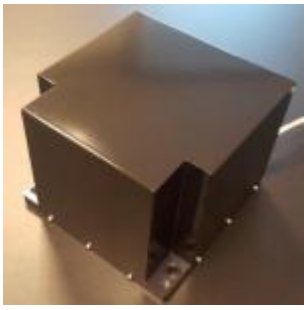	

IFOS-5	IFOS-6	IFOS-10
Inertial measurement unit IFOS-5 is based on Fiber Optical Solution's three axis closed loop fiber optic gyroscope TFOS-5 and three pendulum accelerometers.	Inertial measurement unit IFOS-6 is based on Fiber Optical Solution's three closed loop fiber optic gyroscopes SFOS-6 and three pendulum accelerometers.	High-precision inertial measurement unit IFOS-10 is based on Fiber Optical Solution's three fiber optic gyroscopes SFOS-10 and three pendulum accelerometers.

Table 1.4.2

Momentary characteristics of IMUs based on three pendulum accelerometers

Parameter	**IFOS-5**	**IFOS-6**	**IFOS-10**
Range of measured acceleration, g	±10g to ±40g	±10g to ±40g	±10g to ±40g
Bias drift at constant temperature, mg	≤0.5	≤0.1	≤0.05
Velocity random walk, μg/√Hz	≤20	≤20	≤15
Scale factor error in temperature range -40°C	≤300(*≤100)	≤300(*≤100)	≤100

to +60°C (1σ), ppm			
Physical Characteristics			
Misalignment, °	≤0.08(*≤0.015)		
Output sample rate	up to 2000 Hz		
Power supply, V	5 or 24~36	27±5	27±5
Power consumption, W	≤10 W	≤20 W	≤20 W
Digital output interface	RS-485 or RS-422	RS-422	RS-422
Dimensions, mm	110 × 110 × 90	140 × 140 × 110	171 × 224 × 233

1.5. Introduction to Vibratory MEMS accelerometer

Vibratory or seismic accelerometers are designed specifically to measure sinusoidal accelerations. They find applications in a wide range of fields, including structural testing, earthquake detection, and tsunami monitoring [14]. Fig. 1.5.1 present a vibrating string.

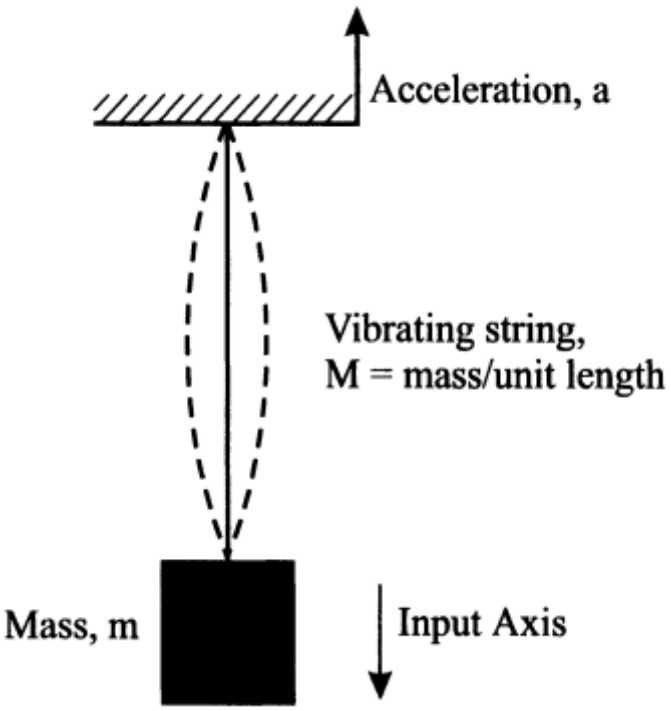

Fig. 1.5.1. A vibrating string

Micromechanical vibrating accelerometers (MMVA) have gained significant attention in recent years due to their unique properties and operational characteristics, which distinguish them from conventional micromechanical capacitive accelerometers (MMCA) currently in use. MMVA offers several advantages, including significantly higher sensitivity, exceeding that of traditional capacitive accelerometers by an order of magnitude, as well as a high dynamic range and stability [15].

The principle of operation

The principle of operation of a vibration MEMS accelerometer involves several key steps:

1. **Vibrating Mass**: The accelerometer contains a mass that is attached to elastic elements, such as a membrane or a beam. When subjected to acceleration, the mass vibrates, causing a change in distance between itself and the stationary part of the device.
2. **Change in Distance**: Acceleration causes the vibrating mass to move relative to the stationary part. For instance, downward acceleration causes the mass to move

upward relative to the stationary part, while upward acceleration causes the mass to move downward.

3. **Change in Capacitance**: The movement of the mass alters the electrical parameters, particularly the capacitance, between the mass and the stationary part. This change in capacitance is directly proportional to the change in distance and serves as a measure of the applied acceleration.

4. **Capacitance Measurement**: The accelerometer incorporates a capacitance sensor designed to detect and measure the change in capacitance resulting from the mass movement. This sensor is often integrated into a MEMS chip and employs various techniques like piezoelectric or liquid-based sensors for precise measurements.

5. **Data Processing**: The changes in capacitance detected by the sensor are converted into an electrical signal. This signal is then processed by the electronic components of the accelerometer to determine the magnitude and direction of the applied acceleration.

By following this operational principle, vibration MEMS accelerometers achieve accurate acceleration measurements with high sensitivity and reliability, making them valuable tools in various applications requiring precise acceleration sensing.

For several years, ONERA has been engaged in the development of two monolithic quartz sensors (Fig. 1.5.2), namely the "VIA" accelerometer (Vibrating Inertial Accelerometer) [16]. The utilization of quartz crystal presents two primary advantages: firstly, it facilitates easy excitation and detection of suitable vibrations through the piezoelectric effect, and secondly, it capitalizes on the highly stable mechanical properties inherent to quartz. Consequently, the incorporation of quartz enables the creation of cost-effective, high-performance vibrating sensors.

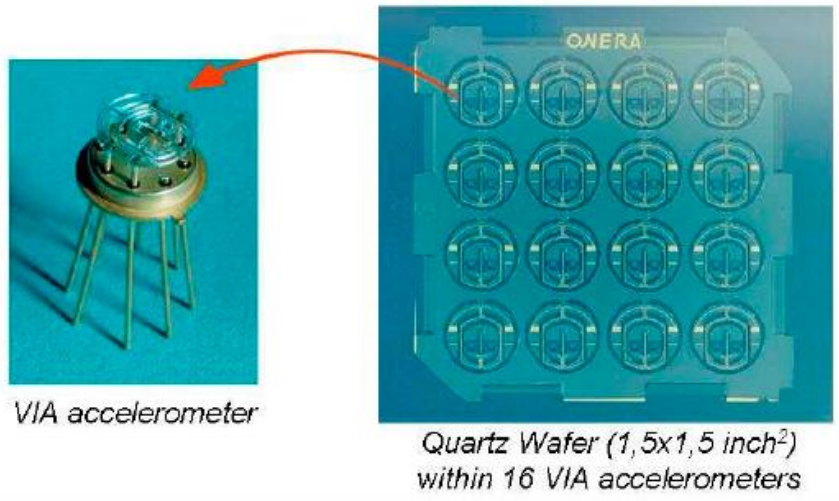

Fig. 1.5.2. Quartz Vibrating Inertial Sensors developed at ONERA

The accuracy of the VIA accelerometer is approximately 300 μg (within a measurement range of ±100g).

Vibrating Beam Accelerometers (VBAs) are particularly attractive for their precision in scale factor accuracy and frequency output. They function by detecting changes in the resonance frequency of a vibrating beam under acceleration, often using a dual-beam configuration to counteract typical parasitic sensitivities like temperature, pressure, and aging. Achieving reliable VBAs requires three key beam insulations:

1. Thermal stress insulation: Thermal variations induce stresses in the structure due to material expansion differences between the quartz and its base. Effective insulation against these stresses is crucial for optimal thermal behavior, minimizing thermal sensitivity and hysteresis.

2. Vibration insulation of the beams: To maintain the high-quality factors of quartz beams and ensure accelerometer stability, minimizing energy losses from the quartz structure is imperative.

3. Insulation between the two beams: Differential VBAs utilize a push-pull configuration with two beams. Consequently, frequency crossover occurs within the measurement range, potentially leading to the "lock-in" phenomenon where mechanical coupling causes a frequency lock and diminishes measurement

accuracy. Hence, substantial insulation between the beams is necessary to reduce the "lock-in" effect and enhance measurement precision [17].

Vibration accelerometers utilizing quartz crystal technology harness the resonance properties of quartz crystals to measure acceleration. The fundamental principle involves two quartz crystal beams attached to separate support masses in a parallel setup (refer to Fig. 1.5.3).

Each quartz beam, referred to as a bundle, resonates at its unique frequency when oscillating along the input axis. When the accelerometer is stationary, these frequencies are identical. However, when acceleration occurs along the axis parallel to the beams (the sensor's sensing axis), one beam compresses while the other stretches.

This discrepancy in the beams' conditions results in frequency changes. The difference between these modified frequencies is directly proportional to the acceleration along the sensing axis. Thus, by measuring the variation in the quartz beams' oscillation frequencies, the accelerometer accurately determines the acceleration affecting the sensor.

The use of quartz crystals enables the creation of highly sensitive and precise accelerometers. Quartz crystals exhibit stable resonant frequencies and demonstrate excellent linearity in frequency change concerning acceleration. These traits make quartz-based sensors ideal for applications requiring meticulous and reliable acceleration measurements. They are extensively utilized in various measurement systems necessitating elevated levels of accuracy and reliability in acceleration sensing [18].

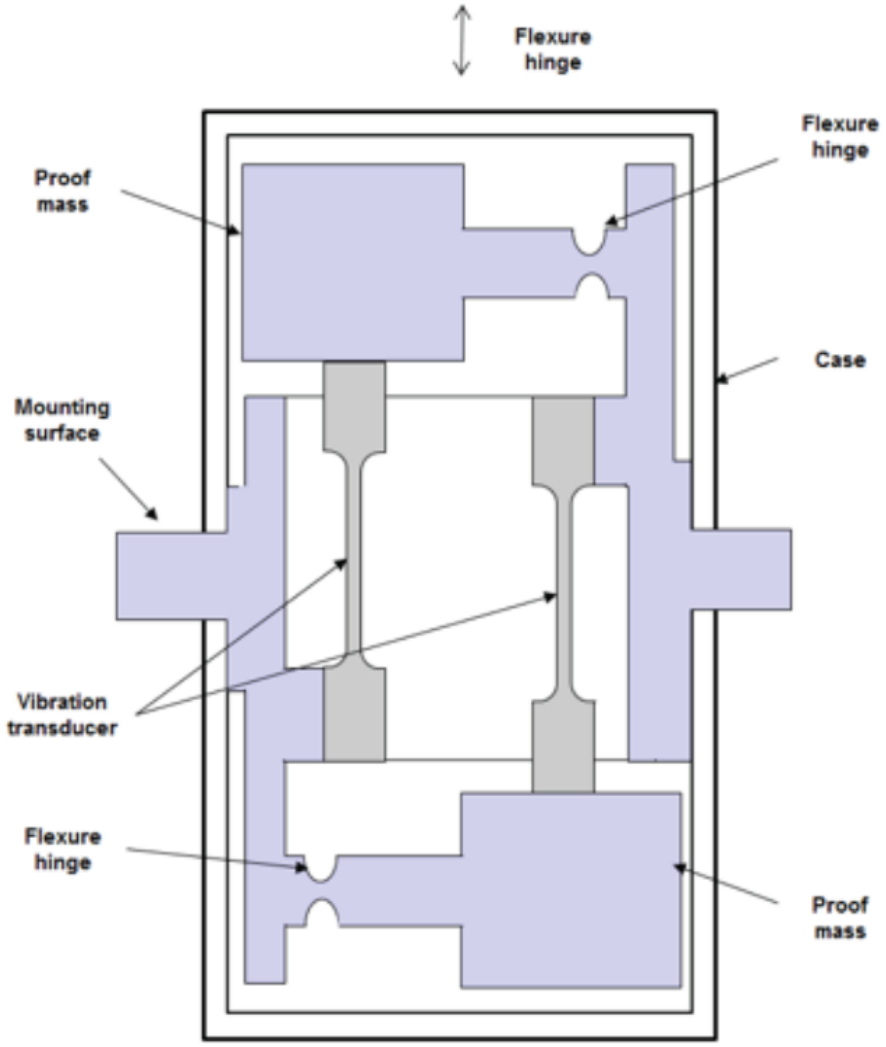

Fig.1.5.3. Vibrating beam accelerometer

Currently, microelectromechanical systems (MEMS) are being manufactured by leading companies in the USA, Japan, Korea, China, and other countries. One notable organization in the USA is the Draper Laboratory, a not-for-profit research and development institution that was among the first to delve into silicon micro-machined capacitive accelerometers (MMCA). The accelerometers developed by Draper Laboratory are known for their exceptional stability, with scaling factors of at least 1 ppm.

In addition to Draper Laboratory, the University of California, Berkeley, has made significant contributions to MEMS technology with their Micromechanical Vibrating Accelerometer (MMVA). This accelerometer boasts a sensitivity of 17 Hz/g

and incorporates dual oscillators to mitigate thermal sensitivity, enhancing its performance in various environments.

Researchers from Seoul National University in South Korea have also made notable strides in MEMS accelerometer development. They have designed a micromechanical resonator silicon accelerometer with a sensitivity of 70 Hz/g and a resonance frequency of 12 kHz, showcasing advancements in sensitivity and frequency response.

Chinese MEMS developers, particularly institutions like Tsinghua University in Beijing, are actively engaged in modeling and prototyping silicon accelerometers. Collaborating with the Institute of Microelectronics, Tsinghua University has produced an MMVA prototype with a sensitivity of 27.3 Hz/g and an impressive resolution of 167.8 μg. This prototype showcases the ongoing advancements in MEMS technology, highlighting the focus on achieving higher sensitivity and resolution while maintaining cost-effectiveness. Additionally, institutions in China, such as Tsinghua University, are contributing significantly to the global landscape of MEMS accelerometers, driving innovation and expanding the capabilities of these sensors across various industries and applications.

Over the past decade, MEMS technologies have witnessed remarkable progress due to their high reliability and cost-effectiveness. These advancements have paved the way for innovative applications across industries, from consumer electronics to aerospace and healthcare, highlighting the continuous evolution and potential of MEMS accelerometers in modern technology.

1.6. Conclusion

Microelectromechanical accelerometers (MEMS accelerometers) therefore encompass a wide range of devices, including pendulum MEMS accelerometers and vibration MEMS accelerometers, each with its own unique operating principle and application. Pendulum MEMS accelerometers use the concept of a pendulum to

measure linear acceleration, offering simplicity and versatility across a variety of industries. Vibration MEMS accelerometers, on the other hand, use the principles of vibration to provide high sensitivity and accuracy for specific applications requiring sinusoidal acceleration measurement.

Numerous manufacturers specialize in the production of MEMS accelerometers, such as Inertial Labs, ENDAQ, Analog Devices Inc. (ADI) and others, contributing to the development of MEMS-based inertial measurement units (IMUs). These IMUs combine MEMS accelerometers with other sensors, such as gyroscopes, to provide comprehensive motion sensing capabilities for applications ranging from consumer electronics to aerospace and defense.

The performance parameters of MEMS accelerometers, including sensitivity, dynamic range, stability and frequency response, play a critical role in determining their suitability for specific applications. Engineers and researchers are constantly striving to improve these parameters to meet the growing demands of industry for accurate and reliable motion measurement solutions.

As such, MEMS accelerometers have revolutionized inertial technology, offering compact, cost-effective and high-performance solutions for a wide range of applications in a variety of industries. Their further development and integration into modern IMUs are making a significant contribution to the development of navigation, robotics, automotive safety systems and many other industries that depend on accurate motion measurement and control.

SECTION 2

THE ALLAN VARIANCE AND RANDOM ERRORS DESCRIPTION

2.1. Introduction to Allan Variance

In the realm of modern science and technology, ensuring the accuracy and stability of sensors and measuring systems is paramount. This necessitates sophisticated methods for analyzing and modeling random errors, which can significantly impact measurement precision.

One standout approach in this domain is Allan's method of variational analysis. It serves as a powerful and widely adopted tool for assessing the variational stability of measurement systems. By employing this method, researchers can delve into the characteristics of random errors within measuring instruments, identify key parameters, and construct models that elucidate their influence on measurement accuracy.

This chapter aims to delve into the intricate world of random error models delineated by the Allan variance curve. Starting with an overview of primary noise and error models, the discussion progresses to their mathematical analysis and subsequent impact on measurement accuracy. Utilizing the Allan analysis of variance method not only aids in pinpointing random errors but also facilitates the formulation of effective strategies to mitigate and rectify these errors.

The core objective of this chapter is to foster a comprehensive understanding of variational stability in measuring systems through the lens of Allan's analysis of variation method. Additionally, it seeks to explore novel approaches to modeling and controlling random errors, thus contributing to advancements in sensor accuracy and stability [19].

The Allan variance is a measure of the variance of the difference between successive samples in a time series, normalized by the time interval between samples. It is defined as the square of the Allan deviation, which is the standard deviation of the differences between adjacent sample values.

One of its key features is that it examines how the variance changes as a function of the averaging time. By averaging over different time intervals, the Allan variance can reveal underlying patterns in the frequency stability of a system.

Random errors, also known as white noise or short-term fluctuations, contribute to the Allan variance. These errors are typically unpredictable and can arise from various sources such as electronic noise, environmental factors, or inherent characteristics of the system.

The Allan variance helps distinguish between different types of errors based on their characteristic time scales. For example:

- Short-term errors (with time scales shorter than the averaging time) contribute to the initial decrease in Allan variance at small averaging times.
- Medium-term errors (with time scales comparable to the averaging time) affect the stability over intermediate averaging times.
- Long-term errors (with time scales longer than the averaging time) become dominant at longer averaging times and may indicate drift or systematic biases.

In summary, the Allan variance is a valuable tool for understanding and quantifying random errors in frequency sources, providing insights into their stability characteristics across different time scales.

2.2. The Allan variance understanding curve and its components

The Allan Variance, named after David W. Allan who developed it, serves as a statistical technique crucial for evaluating the stability and accuracy of clock sources and dynamic systems over time. Initially devised in the 1960s to analyze atomic clock stability, this method has become indispensable across a range of fields, including telecommunications, navigation, and metrology. Its principal function remains assessing clock performance, ensuring precision for devices reliant on accurate timekeeping in modern technology.

This method proves invaluable for measuring RMS random drift errors over varying time spans. Its computational simplicity and straightforward interpretation make it a favored approach for characterizing different types of noise observed in data from inertial sensors. Through specific operations applied to the dataset, the Allan variance method produces a distinctive curve (see Fig. 2.2.1). Analyzing this curve systematically enables a comprehensive understanding of the various random errors inherent in inertial sensor output data.

Mathematically, it is represented as follows:

The Allan Deviation (ADEV), also known as sigma-tau, is the square root of the Allan Variance. Just like standard deviation is the square root of variance, the Allan deviation is the square root of the Allan variance [20]. Mathematically, it is expressed as:

The Allan variance method serves as a valuable tool for quantifying RMS random drift errors concerning average time. Its computational simplicity and straightforward interpretation make it a preferred choice for characterizing different types of noise within inertial sensor data. By applying specific operations across the dataset's entirety, this method generates a distinctive curve. Analyzing this curve systematically enables a thorough characterization of the various random errors inherent in the output data of inertial sensors. [21]

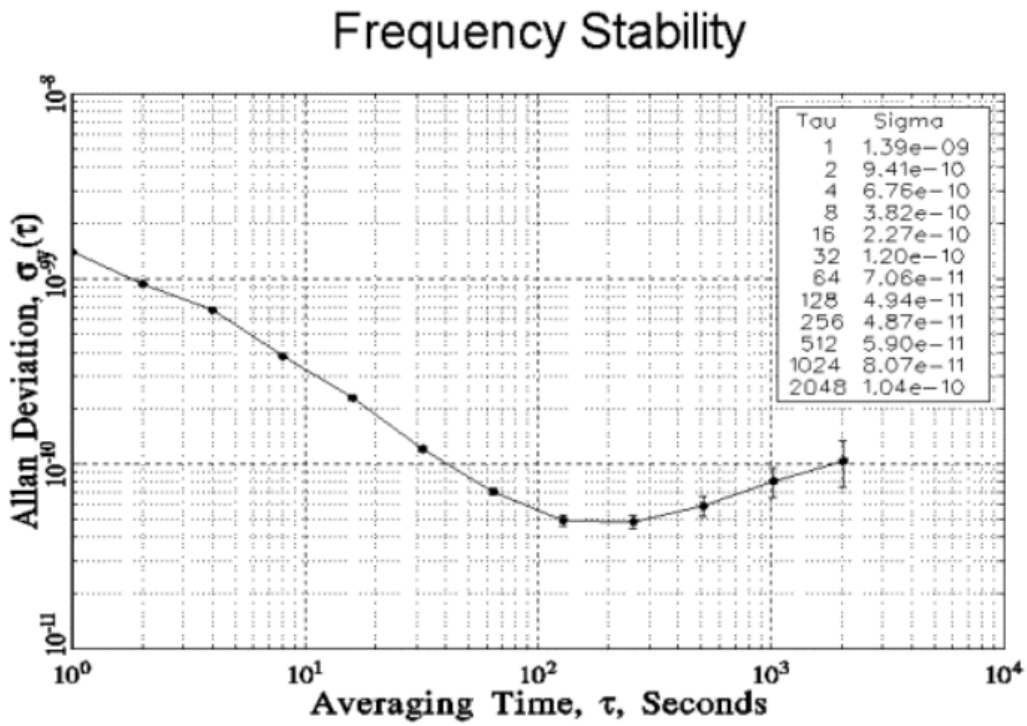

Fig. 2.2.1. Allan deviation curve

The resulting plot is known as the Allan deviation curve, and it typically has a characteristic shape that reveals important information about the stability and accuracy of the oscillator. For short averaging intervals, the Allan deviation is dominated by the short-term noise in the oscillator signal, which causes the variance to increase rapidly as the averaging interval decreases. As the averaging interval increases, however, the noise begins to average out, and the Allan deviation reaches a minimum value, known as the Allan variance floor. This floor represents the fundamental limit on the accuracy and stability of the oscillator and is determined by its underlying physics.

Hence, Allan variance is a powerful tool for measuring the stability and accuracy of oscillators and other time-varying systems. By providing a quantitative measure of the noise and error in these systems, it helps engineers and scientists to optimize their performance and to ensure that they meet the stringent requirements of modern technology. [22]

The Allan variance methodology incorporates cluster analysis in its computation process. Here are the steps involved in computing the Allan variance:

Divide the data stream into clusters of a specified length. If there are N consecutive data points, each with a sample time of t0, form groups of n consecutive data points where n<N/2. Each group member constitutes a cluster, as illustrated in Fig. 2.2.2 [21].

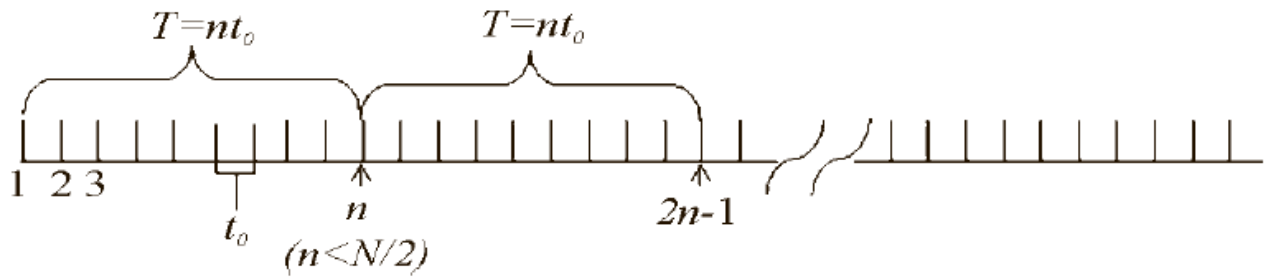

Fig. 2.2.2. Schematic of the data structure used in the derivation of Allan variance

The Allan variance curve and its components

The Allan variance is a key metric used to assess the stability of a clock or oscillator over a specific time period. It's computed by taking half of the time average of the squared deviations between successive frequency readings obtained at regular intervals (the sampling period). Rather than a single value, it's a function reliant on the sample period (often denoted as τ) and the distribution under examination, typically depicted graphically to illustrate data trends.

A low Allan variance indicates good stability of the clock or oscillator over the measured period. It is commonly represented as an Allan deviation plot, usually in a log-log format for clarity and ease of comparison with other error sources. For example, an Allan deviation of at an observation time of 1 second (τ = 1 s) signifies

an instability in frequency between two observations one second apart with a relative root mean square (RMS) value of . For a 10-MHz clock, this translates to an RMS movement of 13 mHz.

It's important to note that if phase stability is required, time deviation variants should be consulted and utilized. Additionally, Allan variance and other time-domain variances can be converted into frequency-domain measures of time (phase) and frequency stability, offering a comprehensive understanding of the system's performance [23].

The Allan variance method offers a detailed depiction of various noise components inherent in inertial sensor data. Below are the fundamental solutions for specific noise terms:

(a) Quantization noise: The Allan variance for quantization noise (Fig. 2.2.3) is given by:

—

where is the quantization noise coefficient;

T is the sample interval.

A log-log plot of σ(T) against T, displaying a slope of -1.

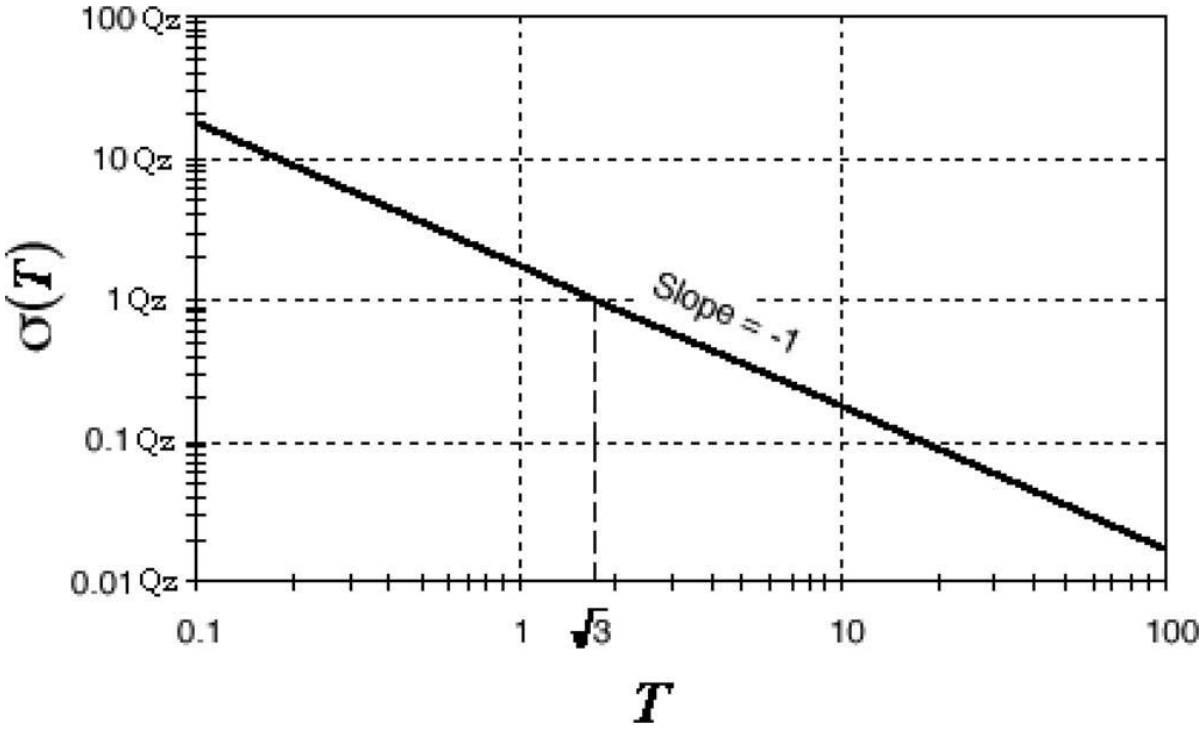

Fig. 2.2.3. $\sigma(T)$ plot for quantization noise

(b) Angle (velocity) random walk (Fig. 2.2.4): This noise arises from high-frequency terms with correlation times much shorter than the sample time. A log-log plot of versus T shows a slope of -1/2. The Allan variance for angle (velocity) random walk is:

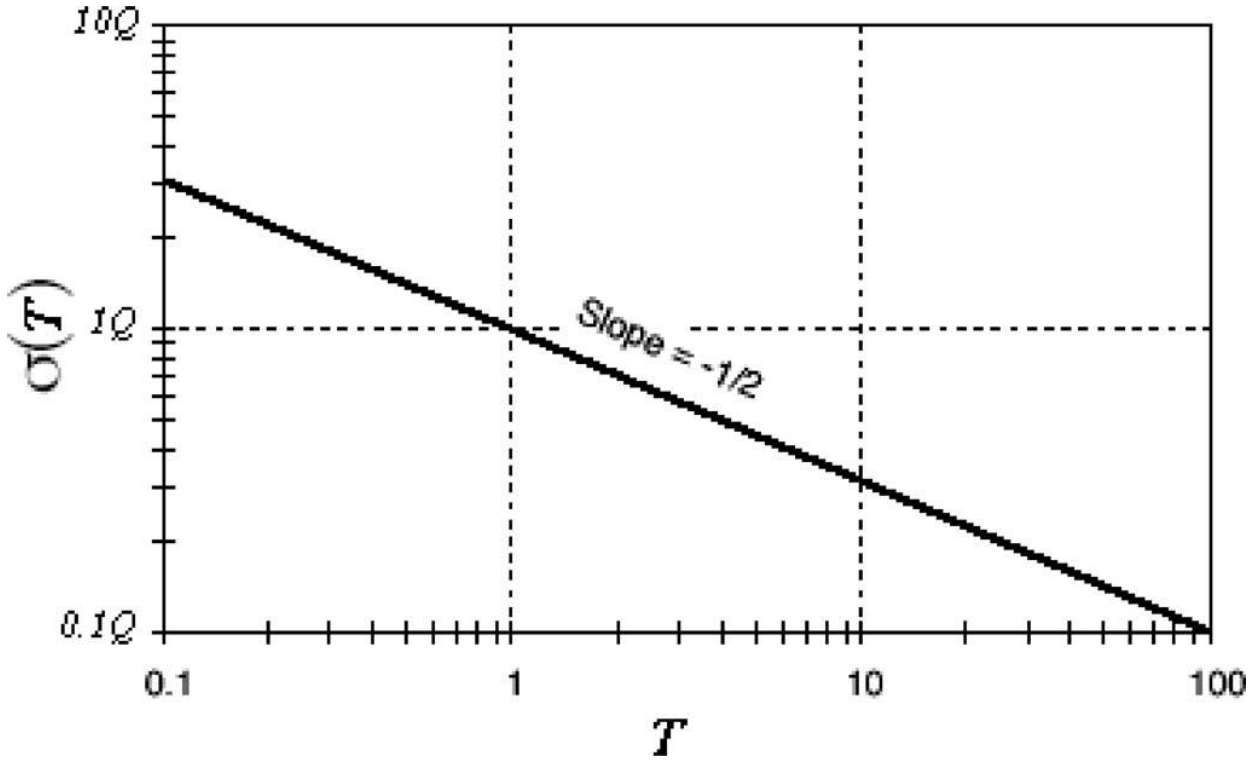

Fig. 2.2.4. $\sigma(T)$ plot for angle (velocity) random walk

(c) Bias instability (Fig. 2.2.5): Originating from electronics or components with random flickering, bias instability manifests as low-frequency bias fluctuations. The bias instability value is determined from the root Allan variance plot where the slope is zero. The Allan variance for bias instability is:

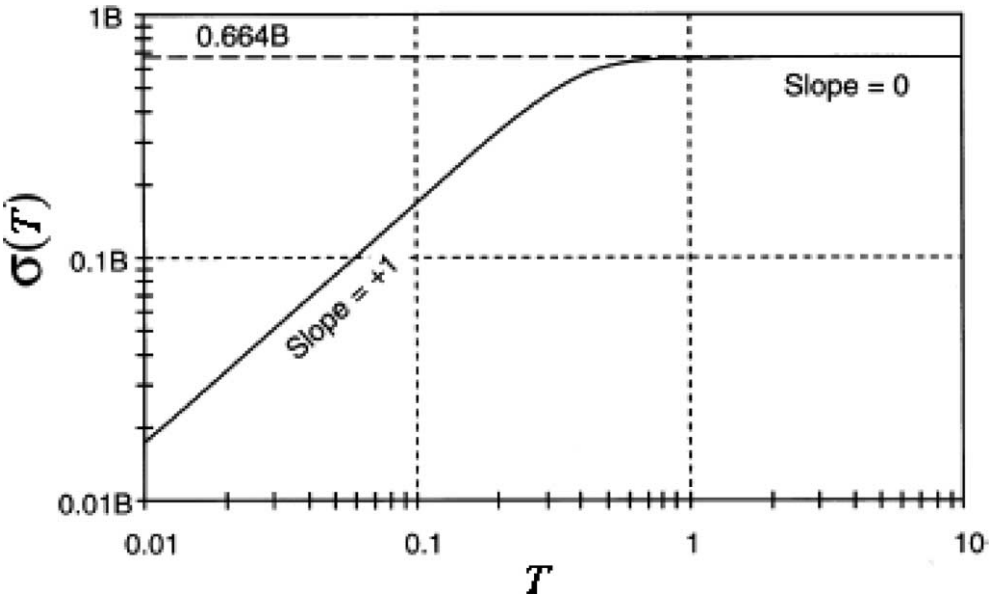

Fig. 2.2.5. $\sigma(T)$ plot for bias instability

(d) Rate random walk (Fig. 2.2.6): Resulting from integrating wideband acceleration PSD, rate random walk's Allan variance is:

$$\sigma^2(T) = \frac{K^2 T}{3}$$

where K is the rate random-walk coefficient. A log-log plot of $\sigma(T)$ versus T shows a slope of +1/2, with K given in units of $\text{unit}/\sqrt{\text{Hz}}$.

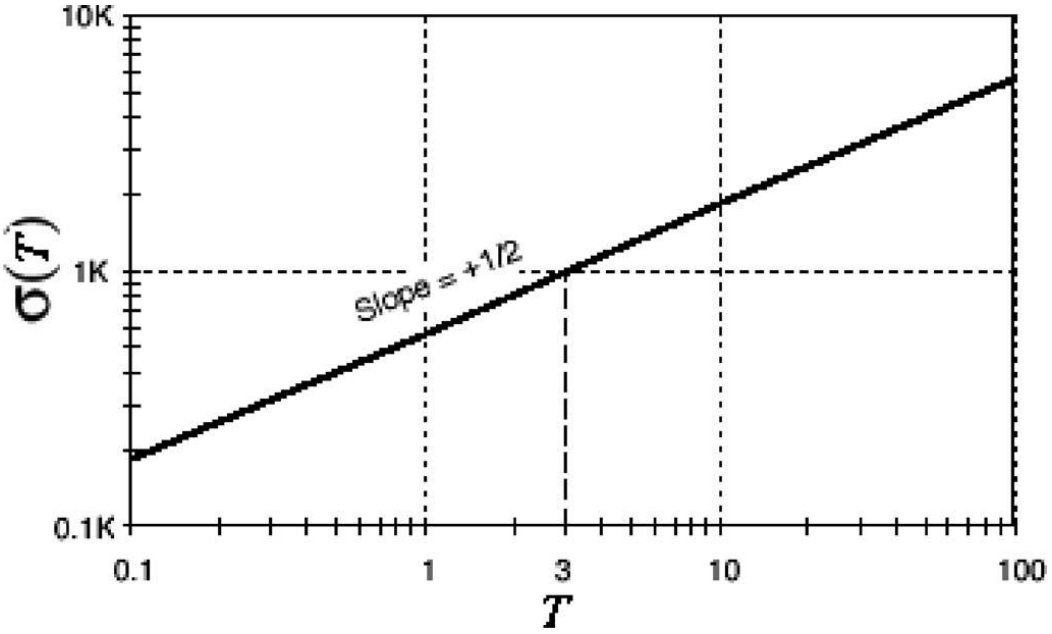

Fig. 2.2.6. $\sigma(T)$ plot for rate random walk

(e) Rate ramp (Fig. 2.2.7): More deterministic than random noise, a log-log plot of $\sigma(T)$ versus T exhibits a slope of +1, rate ramp's Allan variance is:

$$\sigma^2(T) = \frac{R^2 T^2}{2}$$

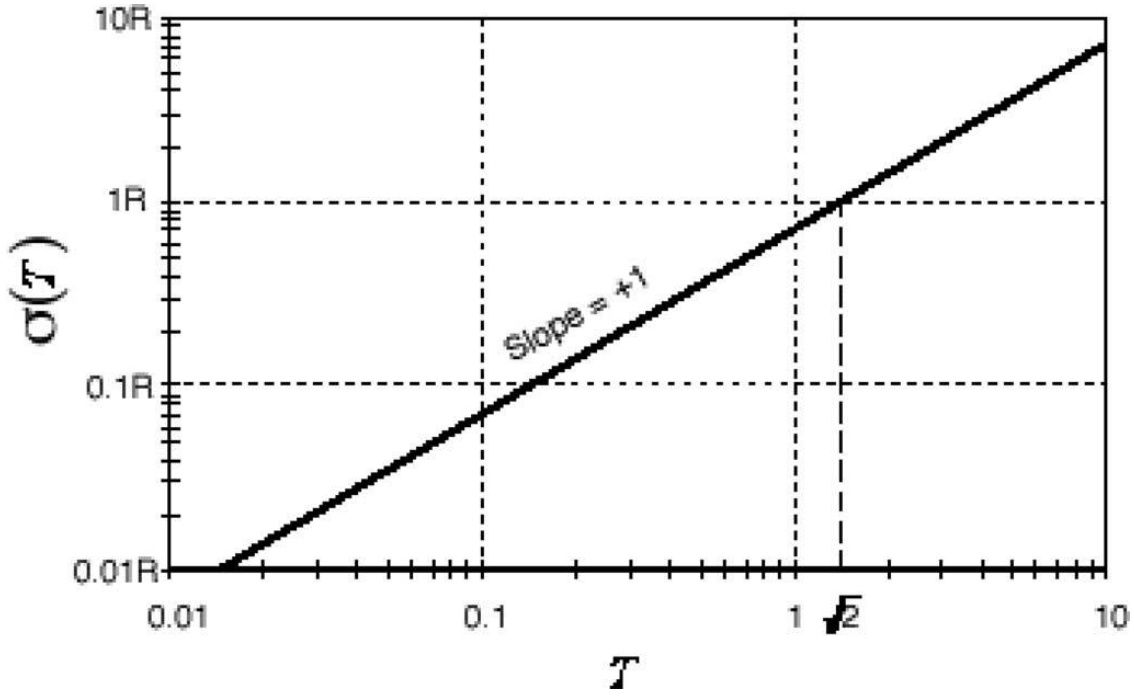

Fig. 2.2.7. $\sigma(T)$ plot for drift rate ramp

The five sources of error, although accurately defined mathematically along the Allan deviation curve using the slope method, require visual inspection of the graph for resolution. This involves creating specific slopes of interest for each parameter, followed by back-solving to estimate their values. This manual process, often necessitated by sensor characteristics and application specifics, underscores the need for careful analysis and human-visual assessment to ensure accurate parameter determination [21][24].

Understanding the Allan Variance Curve

The Allan deviation versus the cluster time (T) is commonly plotted in a log-log graph. Generally, the Allan variance curve is U-shaped. Typically, a range of random processes can manifest within the data, resulting in a varied Allan variance plot akin to the depiction in Fig. 2.2.8. This visual representation facilitates the straightforward identification of different random processes embedded in the dataset. In actual data scenarios, smooth transitions between distinct Allan standard deviation slopes are observable. Additionally, the plot curve may exhibit a degree of noise or irregularity attributed to the inherent uncertainty associated with the measured Allan variance [21].

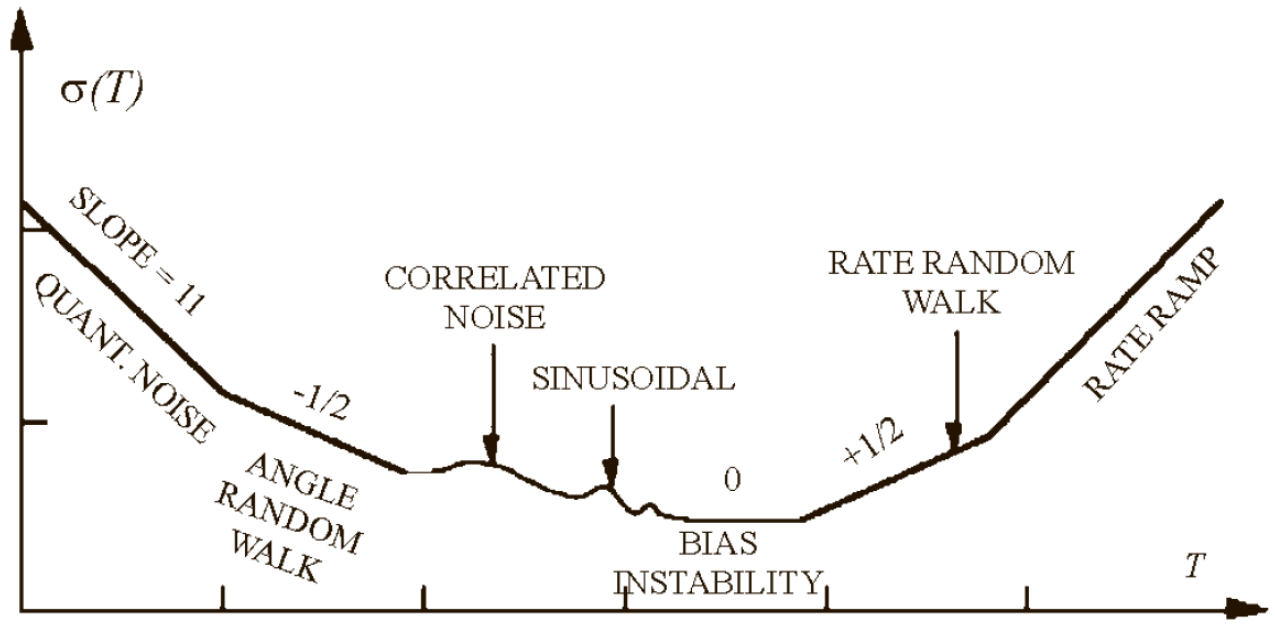

Fig. 2.2.8. Standard form of curve of Allan deviation

The Allan variance plot depicts a spectrum of noise frequencies, with high-frequency noise represented on the left and low frequencies on the right, corresponding to short and long-time intervals, respectively. Quantization noise (QN) appears at the far left of the plot, indicated by a slope of -1. Determining the quantization coefficient involves fitting a line to the data at a specific cluster time, typically t = sqrt(3). This noise component may not always be evident in actual data.

Moving towards the center of the plot, the contribution of white noise becomes apparent, manifested in the gyroscope's angle random walk (ARW) or accelerometer's velocity random walk (VRW). This noise type is associated with a slope of -1/2. Estimating the random walk coefficient involves fitting a line at t = 1 cluster time.

As the curve reaches its minimum, indicating lower frequencies, bias instability (BI) becomes discernible. Bias instability results from low-frequency random fluctuations in electronic components. A line with a slope of 0, fitted to the local minima points and scaled appropriately, reveals the value of bias instability.

Further along the curve, the presence of rate random walk (RRW) can be identified by fitting a line with a slope of +1/2 and determining its intersection at t = sqrt(3). At t = sqrt(2), the +1 slope denotes rate ramp (RR). Exponentially correlated

noise and sinusoidal noise pose challenges in characterization using Allan variance, necessitating careful analysis of consecutive slopes (+1/2 followed by -1/2 for exponentially correlated noise, and repeated +1/-1 slopes for sinusoidal noise) for identification, which can be challenging in practical data analysis.

The Allan variance analysis offers flexibility in selecting units on its horizontal axis (T), ranging from microseconds to hours, depending on the application. On the vertical axis, units represent angular velocity (e.g., rad/s or °/h) for gyroscopes or acceleration (measured in g or m/s^2) for accelerometers.

The slope of the Allan variance curve varies with the cluster time (T), providing insights into the nature of noise in the data. This approach helps identify and quantify different noise terms within the dataset.

Common random errors include quantization noise, angle random walk, bias instability, rate random walk, and rate ramp. Among these, quantization noise, bias instability, and rate random walk often have the most significant impact on gyroscope output accuracy and stability.

The analysis of the Allan Variance curve involves delineating its three key segments. The initial segment of the curve displays a negative slope from the starting point, denoted as σ, to points near the minimum. Each point, represented as σ^2 (1), signifies the deviation or variance within a set of averaged values derived from the dataset. For instance, the second point on the curve corresponds to the averaged values of consecutive pairs (x_m + x_(m+1))/2 for all in ℕ. Averaging over two samples attenuates the highest frequency noise components, resulting in a lower deviation represented by the second point compared to the first, and similarly, the third point exhibits reduced deviation from the second, and so on.

The middle segment of the Allan Variance curve covers the vicinity of the minimum point. Ideally, one would expect that increasing the number of samples for averaging would progressively diminish the variance and deviation of the averaged samples, approaching zero in an exponential manner. However, in systems with non-

convergent noise, this reduction does not occur as anticipated due to various factors contributing to this divergence.

The final segment of the Allan Variance curve encompasses the region where the slope becomes positive, ascending from the minimum point. This ascent is primarily attributed to the growing influence of 1/f noise and other low-frequency noise sources such as random walk at low frequencies and extended sampling times. When sample averages are computed over very low frequencies but less than a full cycle, they demonstrate a range of values spanning from the maximum amplitude of the low-frequency components to the minimum. This variability across a band of low frequencies contributes to a measurable noise distribution, resulting in the observed rise in the Allan Variance curve.

The total measurement time Tmeas involves collecting or calculating n samples over a specific duration. This period is divided into intervals determined by the constant sampling time Ts, with the maximum number of time-averaged samples ns being ns = Tmeas / Ts.

Increasing the sampling time Ts decreases the high-frequency cutoff of the algorithmic low-pass filter, resulting in more effective averaging of higher frequency noise components for convergent noise.

For the shortest sample averaging time T1, the noise contributing to the Allan deviation includes all frequency components limited by the sample averaging time. However, for s > 1, higher frequencies are progressively averaged away, resulting in the variance due to noise being primarily composed of lower frequency components.

The two-sample deviation measures the deviation between successive averaged samples, capturing noise frequencies equal to or greater than 1/(two sample periods + any dead time). Lower noise frequencies of interest lead to smaller two-sample deviations, while lower sampling frequencies for a given noise frequency of interest result in greater deviations.

1/f noise exhibits an inverse relationship between amplitude (or power) and frequency. Thus, the two-sample deviation increases as the sampling period increases or as the sampling frequency falls.

There is a low-frequency cut-off determined by Tmeas, where frequencies significantly lower than 1/(Tmeas x 4) contribute minimally to signal deviation due to their slow-changing nature.

The variance of low-frequency noise becomes significant on long timescales, especially in systems exhibiting 1/f noise. This variance grows with increasing Tmeas, highlighting the importance of considering non-convergent noise sources in systems with very slow-changing time-dependent characteristics, such as oscillators responding to temperature variations or gravimeters affected by celestial motions [26].

2.3. Allan Variance Method for Accelerometer Data

A graph of a function (Allan variance) built by measurement data in log-log scale indicates a type of random component, which is in the gyro output signal. It is usually built a graph of a square root of the Allan variance $\sigma_\Omega(T)$ versus a length of time interval T (i.e. averaging time) on a log-log scale.

Different noise components appear on the Allan variance graph at different intervals of the averaging time variable T. This allows one to detect on the Allan curve various random components which are present in the measurement data. Assuming that the above noise components are independent of each other, the total Allan variance can be written as the sum of the variances of its components as follows:

Q is a random drift due to quantum (quantization) noise measured in

(it is present only for digital accelerometers);

N is a random drift due to velocity random walk measured in

B is a random drift due to bias instability measured in

K is a random drift due to acceleration random walk measured in

R is a random drift due to acceleration drift ramp measured in

The *Q* value is determined as an ordinate of an intersection point of a tangential line with slope to curve and a vertical line originating from the point $T=3^{1/2}h$ (hour). Its dimension is g*h, when accelerometer output signal is in g and in g/Hz, when accelerometer output signal is in m/s^2. If Q value for $T=3^{1/2}$h is located out of graph frame, then $T=3^{1/2}\,s$ can be taken and, in this case, *Q* dimension is g/√Hz or in $m/s^2/Hz$.

The *N* value is determined as an ordinate of an intersection point of a tangential line with a slope to curve and a vertical line originating from the point $T=1h$. Its dimension is g/√h, when accelerometer output signal is in g and in $(m/s^2)/\sqrt{h}$, when accelerometer output signal is in m/s^2. If *N* value for $T=1$h is located out of graph frame, then $T=1\,s$ can be taken and, in this case, *N* dimension is $m/s^2/Hz$,

when accelerometer output signal is in m/s^2 or in $g/\sqrt{s}$, when accelerometer output signal is in g.

The *B* value is determined as an ordinate of a minimum of a curve (it's flat part) divided by a constant . Its dimension is g, when accelerometer output signal is in g, and in m/s^2, when accelerometer output signal is in m/s^2.

The *K* value is determined as an ordinate of an intersection point of a tangential line with a slope of to curve and a vertical line originating from the point $T=3\ h$. Its dimension is $g/\sqrt{h}$, when accelerometer output signal is in g, and in $m/s^2/\sqrt{s}$, when accelerometer output signal is in m/s^2. If *K* value for $T=3$ h is located out of graph, then $T=3\ s$ can be taken, and in this case, *K* dimension is $g/\sqrt{s}$, and in $m/s^2/\sqrt{s}$, when accelerometer output signal is in m/s^2.

The *R* value is determined as an ordinate of an intersection point of a tangential line with a slope to curve and a vertical line originating from the point $T=2^{1/2}\ h$. Its dimension is g/h, when accelerometer output signal is in g, and in $m/s^2/h$, when accelerometer output signal is in m/s^2. If *R* value for $T=2^{1/2}$ h is located out of graph, then $T=2^{1/2}\ s$ can be taken, and in this case, *R* dimension is g/s, when accelerometer output signal is in g, and in $m/s^2/s$, when accelerometer output signal is in m/s^2.

As a practical example, let us consider the data that was collected for eight hours of the MMA8451Q MEMS accelerometer of NXP company presented in Fig. 2.3.1.

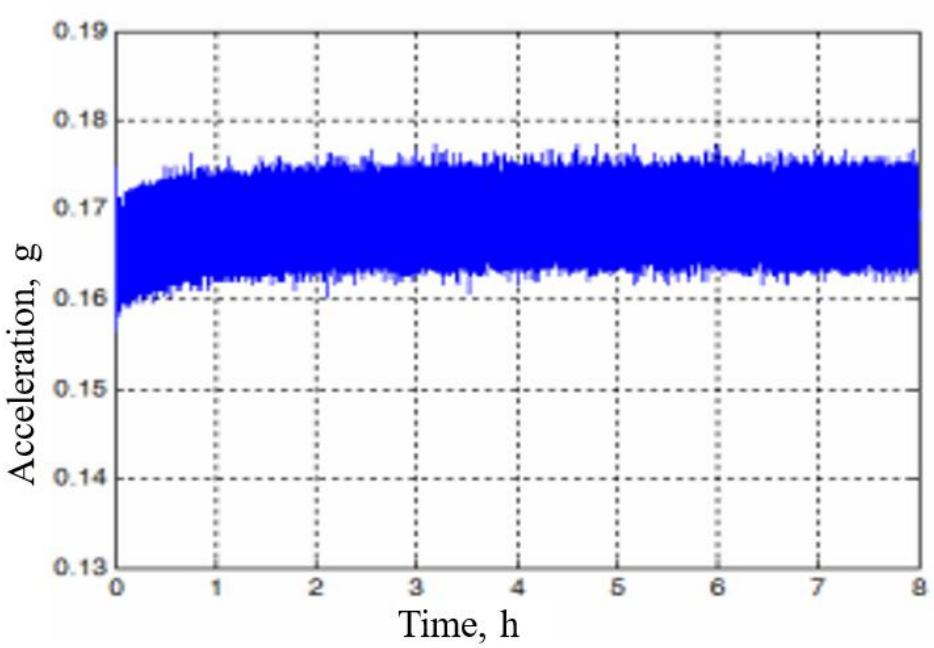

Fig. 2.3.1. The measured accelerometer bias drift.

The orientation of the accelerometer was such that its sensing axis was not aligned with Earth gravity, and was unchanged. Thus, this will not influence on accelerometer noise components analysis.

Allan standard deviations for the data presented in Fig. 2.3.1, is depicted in Fig. 2.3.2.

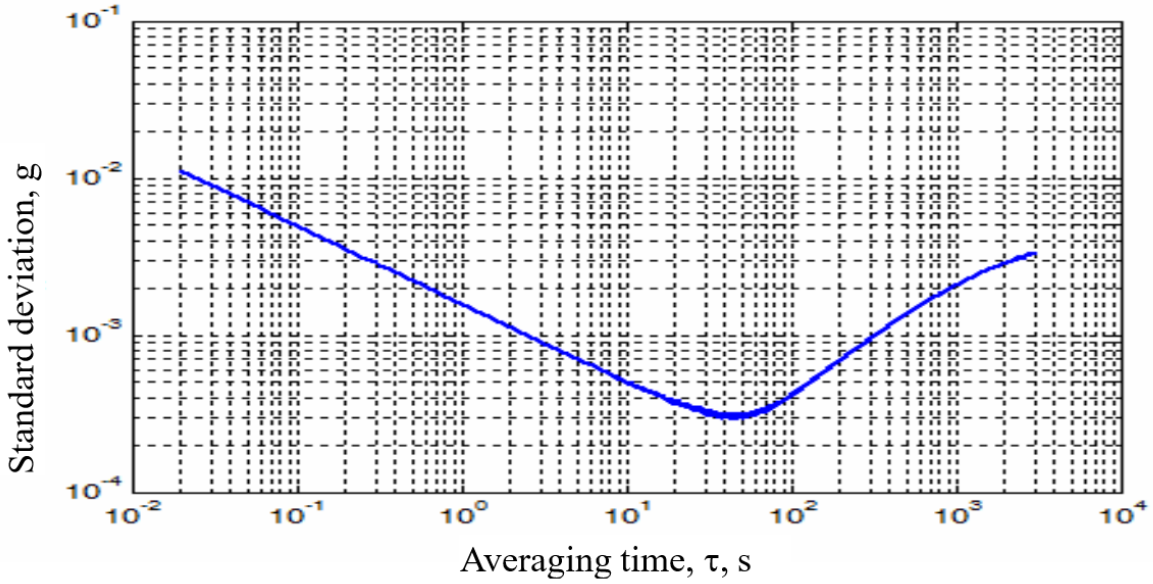

Fig. 2.3.2. Allan standard deviations of accelerometer data

This Allan curve does not contain quantum (quantization) noise or it is too small relative to others because there is not a part of the Allan curve with tilt angle equal to .

Example of velocity random walk noise coefficient *N* determination in correspondence to abovementioned description is presented in Fig. 2.3.3. It is equal to —

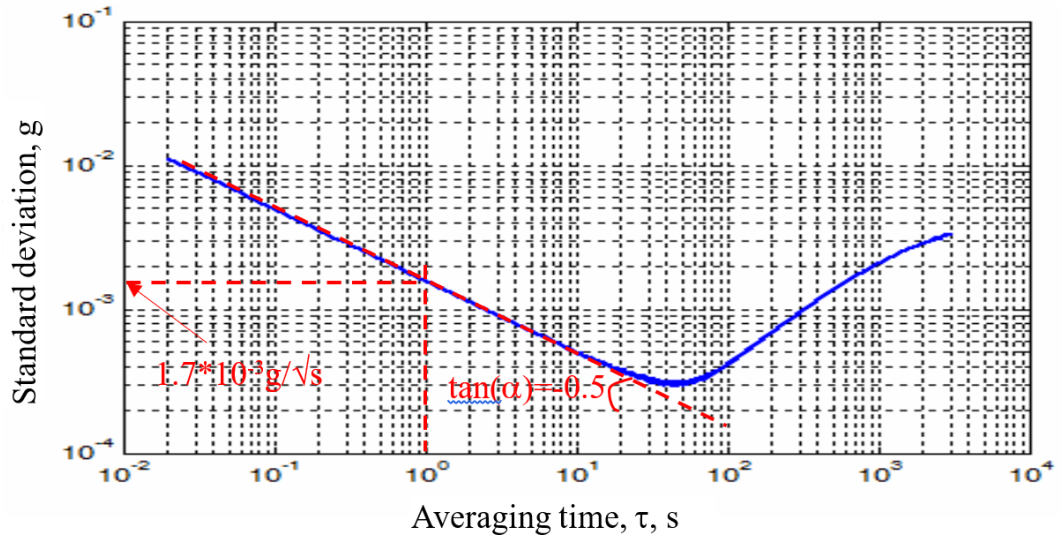

Fig. 2.3.3. Determination of velocity random walk for accelerometer

Example of a bias instability coefficient *B* determination in correspondence to abovementioned description is presented in Fig. 2.3.4. It is equal to

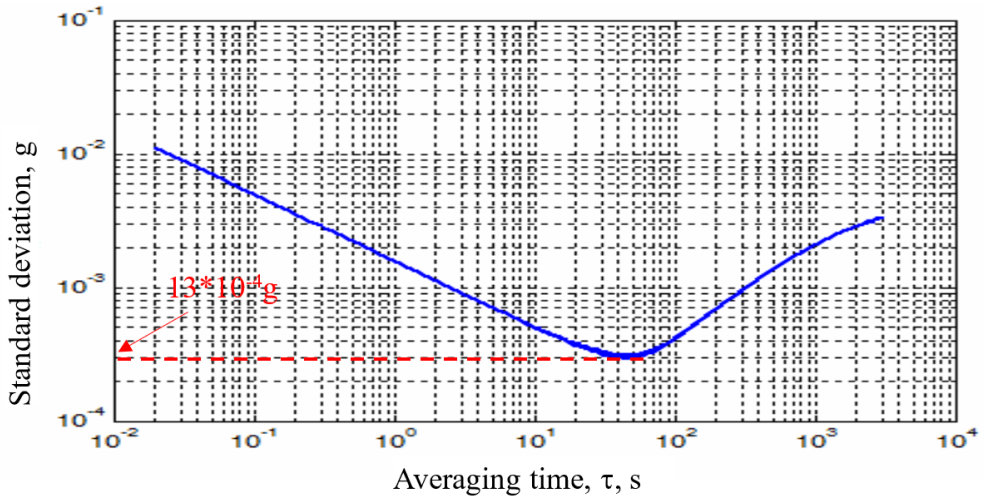

Fig. 2.3.4. Determination of accelerometer bias instability

Example of an acceleration random walk coefficient K determination in correspondence to abovementioned description is presented in Fig. 2.3.5. It is equal to

—

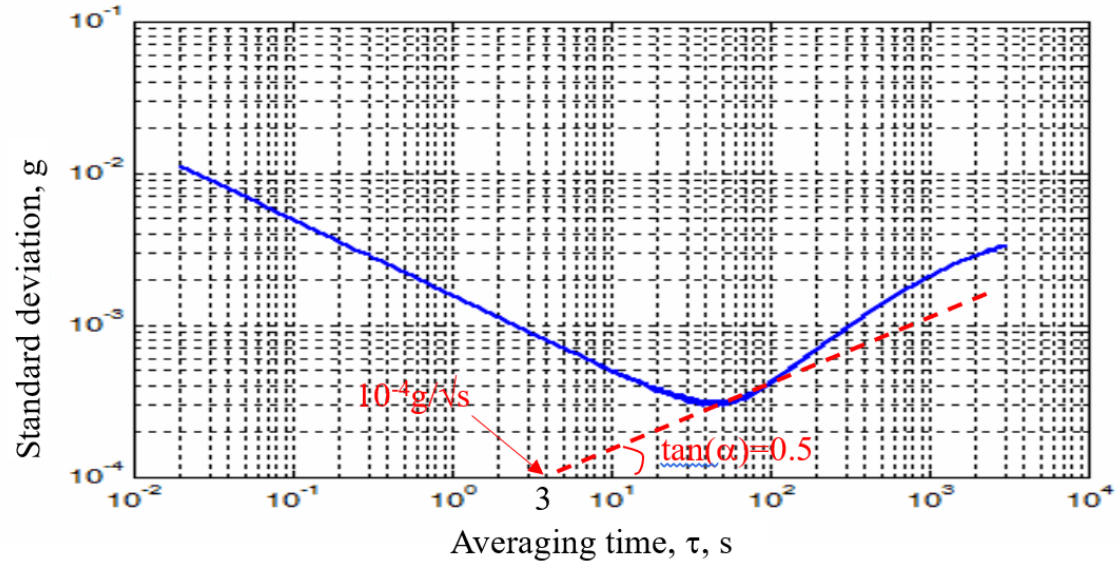

Fig. 2.3.5. Determination of acceleration random walk for accelerometer

Example of an acceleration drift ramp coefficient R determination in correspondence to abovementioned description is presented in Fig. 2.3.6. It is equal to

–

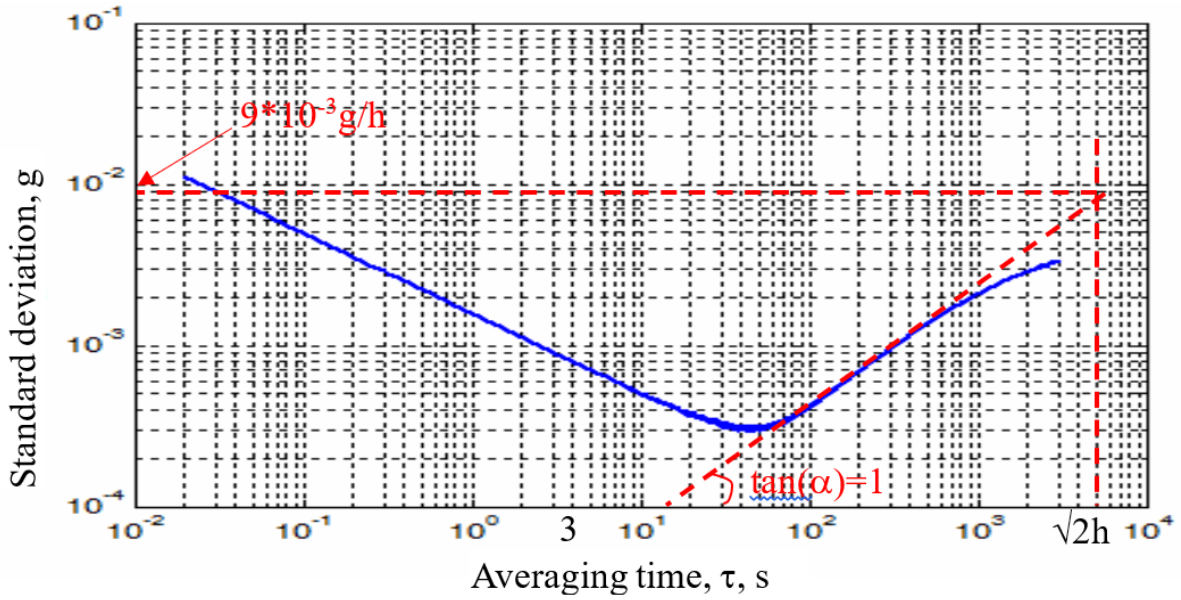

Fig. 2.3.6. Allan standard deviations of accelerometer data

There can be other noises in acceleration data such as exponentially correlated noise, sinusoidal noise; however, this accelerometer data has not such noises [27][28][29].

2.4 Application the Allan variation analysis to MEMS accelerometers

Measuring accelerometer dynamic range from seismic data using Allan deviation involves several steps and considerations:

1. **Data Acquisition:** Obtain seismic data using accelerometers. Ensure that the data acquisition system is calibrated and properly configured to capture a wide range of seismic vibrations.
2. **Preprocessing:** Preprocess the seismic data to remove any noise or artifacts that may affect the accuracy of the analysis. This may include filtering, noise reduction, and data cleaning techniques [28].
3. **Segmentation:** Divide the seismic data into segments or windows of equal duration. The size of the segments will depend on the specific characteristics of the seismic signals and the desired analysis resolution.
4. **Allan Deviation Calculation:** Calculate the Allan deviation for each segment of seismic data. The Allan deviation is a statistical measure that quantifies the variance of a signal as a function of averaging time. It helps in characterizing the dynamic range and noise characteristics of the accelerometer.
5. **Plotting and Analysis:** Plot the Allan deviation results on a graph with the averaging time (tau) on the x-axis and the Allan deviation on the y-axis. Analyze the graph to identify different regions that represent noise-dominated, signal-dominated, and other characteristics of the accelerometer's dynamic range.
6. **Dynamic Range Determination:** Determine the dynamic range of the accelerometer based on the Allan deviation graph. The dynamic range represents

the range of amplitudes or accelerations that the accelerometer can accurately measure without saturating or losing sensitivity [29].

7. **Validation:** Validate the dynamic range measurement by comparing it with specifications from the accelerometer datasheet or known calibration standards. Ensure that the measured dynamic range aligns with the expected performance of the accelerometer under seismic conditions.

8. **Interpretation:** Interpret the Allan deviation results in the context of seismic data and the specific application requirements. Consider factors such as sensitivity, noise floor, resolution, and maximum measurable acceleration when interpreting the dynamic range measurement.

9. **Navigation accuracy:** the application of Allan variance analysis to MEMS accelerometers is instrumental in enhancing navigation accuracy by identifying and mitigating noise-related issues that can impact the reliability and precision of navigation systems [30].

SECTION 3

APPLICATION OF THE ALLAN VARIANCE METHOD TO HIGH ACCURATE QUARTZ ACCELEROMETER

3.1. Allan variance computation algorithm

In today's world, measuring the accuracy and stability of signals is crucial in many fields of science and technology, especially in telecommunications, navigation, and metrology. These fields often demand high precision and stability from signals. This is particularly relevant for systems relying on precise time and frequency measurements, such as GPS, high-frequency trading in financial markets, telecommunications networks, and scientific experiments involving the measurement of fundamental physical constants. Traditional methods of assessing signal stability, such as standard deviation, are not always effective for analyzing signals with time-dependent fluctuations. In such cases, Allan deviation is applied, providing a more adequate assessment of signal stability under various types of noise.

The object of this study is the Allan deviation calculation algorithm, which is used to assess the stability of frequency signals and time series. Allan deviation is a powerful tool that allows separating different noise components in frequency signals and time series, making it indispensable in many technical and scientific applications.

The method of time-domain analysis using Allan deviation, was created for assessing the stability of frequency and phase oscillators. This approach gained wide recognition from IEEE for its ability to analyze parameters of gyroscopes and accelerometers. By effectively isolating various sources of noise, Allan deviation accurately determines their characteristic parameters [34].

Let us remind of key concepts:

Allan Deviation. Defined as half of the mean square difference between consecutive frequency deviation measurements taken over the sampling period. It depends on the time between samples and is typically represented graphically.

Allan Deviation. Is the square root of the Allan deviation and is commonly used for plotting and presenting results as it provides relative amplitude stability, allowing for easy comparison with other error sources.

Analysis of Allan Deviation

1. **Allan Deviation Calculation:**
    - Compute the Allan deviation for a noise sequence using the corresponding formula.
2. **Logarithmic Transformation:**
    - Apply logarithmic transformation to determine the slope of the curve for a specific time τ, creating a double-logarithmic curve.
3. **Identification of Noise Types:**
    - The curve helps identify five types of noise: quantization noise, random walk (angle) noise, bias instability, random walk (rate) noise, and rate ramp.
    - By studying the different slopes for each type of noise, it's possible to estimate when errors may occur.
4. **Reading Intersection Points:**
    - Read the intersection points of tangents for each type of noise with the y-axis, allowing accurate calculation of error coefficients by comparing these points with noise coefficients [34].

Explanation

1. Data Collection:

- Collect data with uniformly distributed time values along with measurements of gyroscopic (or other device) output values, measured in angle/time units (e.g., degrees/second).

2. Interval Partitioning:

- Determine the averaging duration ( ).

- Divide the input data into intervals of duration ( ). For example, if (= 2) seconds and there are 4000 seconds of data, there will be 2000 intervals of 2 seconds each.

3. Calculation of Mean Values:

- Compute the mean value of the gyroscope for each interval ( ). If N is the number of intervals, the mean value for the i-th interval denoted is $a(\tau)_i$:

$$\bar{a}$$

4. Calculation of Differences between Adjacent Intervals:

- Compute the difference between the mean values of adjacent intervals:

5. Calculation of Allan Deviation:

- Calculate the mean value of the squares of the differences between adjacent intervals:

$$\overline{\qquad\qquad}$$

Limitations for Correct Calculation [35]

For correct calculation of the Allan deviation, it's important to adhere to certain conditions:

1. Minimum number of values in each interval:

- Each interval of duration should contain at least 9 measurement values:

2. Minimum number of intervals:

- The entire dataset should contain at least 9 intervals of duration :

Transformation to Allan Deviation

For ease of interpretation of results, Allan Deviation (AD) is often used, which is the square root of Allan deviation:

$$\sqrt{\quad}$$

You may also want to consider fast algorithms to evaluate AVAR of both regularly (Fig. 3.1.1) and irregularly (Fig. 3.1.2) sampled data are presented in this section [36].

Algorithm 1 FAVAR

1: Truncate the data $\{y_i\}$ $(i = 1, 2, \ldots, n)$ to one greater than the nearest integer power of 2 to yield data length $N = 2^p + 1$ $(p \in \mathbb{Z}^+)$.
2: Set the initial window length $m = 2$.
3: Initialize the vector $\mathbf{v}$ and its length l_v:
4: $\mathbf{v} = [y_{n-N+1}\ y_{n-N+2}\ \cdots\ y_{n-1}]^T$
5: $l_v = N - 1$
6: **while** $m \leq 2^{p-1}$ **do**
7: Update $\mathbf{v}$ and l_v:
8: $\mathbf{v} \leftarrow 0.5 \cdot ([v_1\ v_2\ \ldots\ v_{l_v - \frac{m}{2}}]^T + [v_{\frac{m}{2}+1}\ v_{\frac{m}{2}+2}\ \ldots\ v_{l_v}]^T)$
9: $l_v \leftarrow l_v - \frac{m}{2}$
10: Update the vectors $\mathbf{v}^f$ and $\mathbf{v}^b$:
11: $\mathbf{v}^f = [v_{m+1}\ v_{m+2}\ \ldots\ v_{l_v}]^T$
12: $\mathbf{v}^b = [v_1\ v_2\ \ldots\ v_{l_v - m}]^T$
13: Calculate AVAR for a window length m:
14: $\sigma_A^2[m] = \frac{1}{2(N-2m)} \sum_{j=1}^{l_v - m} (v_j^f - v_j^b)^2$
15: Update window length:
16: $m \leftarrow 2m$
17: **end while**

Fig. 3.1.1. Fast algorithm to evaluate AVAR of regularly sampled data

Algorithm 2 FAVAR-I

Truncate the processed data $\{\bar{\theta}_i, w_i\}$ $(i = 1, 2, \ldots, n)$ to one greater than the nearest integer power of 2 to yield data length $N = 2^p + 1$ $(p \in \mathbb{Z}^+)$.
Set the initial window length $m = 2$.
Initialize the vectors $\mathbf{v}$, $\mathbf{w}$ and their length l_v:
$\mathbf{v} = [\bar{\theta}_{n-N+1}\ \bar{\theta}_{n-N+2}\ \ldots\ \bar{\theta}_{n-1}]^T$
$\mathbf{w} = [w_{n-N+1}\ w_{n-N+2}\ \ldots\ w_{n-1}]^T$
$l_v = N - 1$
while $m \leq 2^{p-1}$ **do**
    Update $\mathbf{w}$, l_v, and $\mathbf{v}$:
    $\mathbf{s} = [w_1 v_1\ w_2 v_2\ \ldots\ w_{l_v - \frac{m}{2}} v_{l_v - \frac{m}{2}}]^T +$
    $[w_{\frac{m}{2}+1} v_{\frac{m}{2}+1}\ w_{\frac{m}{2}+2} v_{\frac{m}{2}+2}\ \ldots\ w_{l_v} v_{l_v}]^T$
    $\mathbf{w} \leftarrow [w_1\ w_2\ \ldots\ w_{l_v - \frac{m}{2}}]^T +$
    $[w_{\frac{m}{2}+1}\ w_{\frac{m}{2}+2}\ \ldots\ w_{l_v}]^T$
    $l_v \leftarrow l_v - \frac{m}{2}$
    $\mathbf{v} = [\frac{s_1}{w_1}\ \frac{s_2}{w_2}\ \ldots\ \frac{s_{l_v}}{w_{l_v}}]^T$
    Update the vectors $\mathbf{v}^f$, $\mathbf{w}^f$, $\mathbf{v}^b$, and $\mathbf{w}^b$:
    $\mathbf{v}^f = [v_{m+1}\ v_{m+2}\ \ldots\ v_{l_v}]^T$
    $\mathbf{w}^f = [w_{m+1}\ w_{m+2}\ \ldots\ w_{l_v}]^T$
    $\mathbf{v}^b = [v_1\ v_2\ \ldots\ v_{l_v - m}]^T$
    $\mathbf{w}^b = [w_1\ w_2\ \ldots\ w_{l_v - m}]^T$
    Calculate total weights and AVAR for a window length m:
    $w[m] = \sum_{j=1}^{l_v - m} w_j^f w_j^b$
    $\sigma_A^2[m] = \frac{1}{2w[m]} \sum_{j=1}^{l_v - m} w_j^f w_j^b (v_j^f - v_j^b)^2$
    Update window length:
    $m \leftarrow 2m$
end while

Fig. 3.1.2. Fast algorithm to evaluate AVAR of irregular sampled data

Non-Overlapping and Overlapping Allan Variance

Allan variance (AVAR) calculates the root mean square value of the random drift error as a function of averaging time. The graph of AVAR reveals not only the averaging time that minimizes noise variance but also provides information about different random processes contributing to the drift at the circuit output.

AVAR was first used to measure the frequency stability of precision oscillators and is now widely used in other applications, such as analyzing random errors in MEMS gyroscopes. For gyroscopes, AVAR gives the root mean square random drift error as a function of averaging time.

There are different versions of AVAR, including non-overlapping and overlapping Allan variance, which are commonly used to analyze random errors in inertial sensors.

Non-Overlapping Allan Variance

To calculate the non-overlapping Allan variance, we collect a large number of samples from the gyroscope when it is motionless. Suppose we have a dataset of N samples from the gyroscope output $\Omega(t)$ at multiples of the sampling time . The N samples are divided into K disjoint groups of equal length, where each group (or cluster) has n samples. If the sampling time is , the total time duration of each group is $T=n$.

Example

For $n=3$, each cluster has a time duration of 3 . The first cluster ($k=1$) includes the first 3 samples at , 2 , and 3 . The second cluster ($k=2$) includes the samples at 4 , 5 , and 6 , and so on. To find the Allan variance, we calculate the average of each cluster, denoted by $\Omega k(T)$.

The Allan variance is then calculated using the following equation:

where K is the total number of clusters.

Overlapping Allan Variance

The overlapping Allan variance tends to perform better for large datasets (large *N*). Similar to the non-overlapping version, the *N* samples from the gyroscope output Ω(*t*) are divided into *K* groups of equal length where each group has *n* samples. However, in this case, the clusters overlap.

Example

For *n*=3, the first cluster (*k*=1) includes the first 3 samples at , 2 , and 3 . The second cluster (*k*=2) includes the samples at 2 , 3 , and 4 , and so on. Thus, the clusters overlap.

The average of the *k*-th cluster is denoted by Ω*k*(*T*). The overlapping Allan variance is calculated using:

For *n*=3, the first term of the summation (k = 1) involves the cluster averages Ω1 (*T*) and Ω4(*T*). The next term of the summation (k = 2) involves Ω2(*T*) and Ω5(*T*).

Finally, taking the square root of the result from either equation, we obtain the Allan deviation for a particular value of *T* [37].

3.2. Research on the effect of temperature on the Sagem accelerator: analysis of the collected Z-axis acceleration data

In this assignment, we examine the Sagem accelerator's temperature and Z-axis acceleration measurements. In Fig. 3.2.1 shows an example of a quartz pendulum accelerometer. First, we will look at the temperature profile of the Sagem accelerator in the range of -15 ℃ to +45 ℃, as shown in Fig. 3.2.2. Next, we will look at the collected Z-axis acceleration data for five and a half hours, which is also shown in Fig. 3.2.3. Our

goal is to calculate and plot the curve for the Z-accelerator and determine (from the graphs) the error components available for it.

Fig. 3.2.1. Quartz pendulum accelerometer

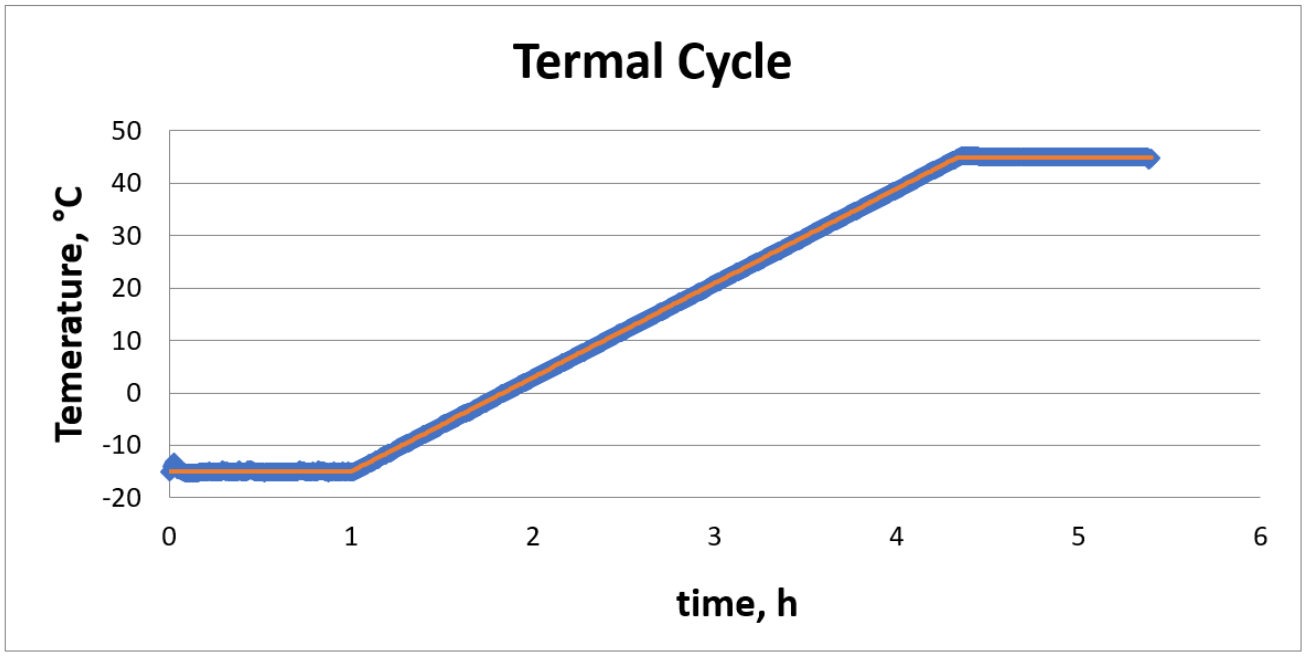

Fig. 3.2.2. Thermal cycle for Sagem accelerometer

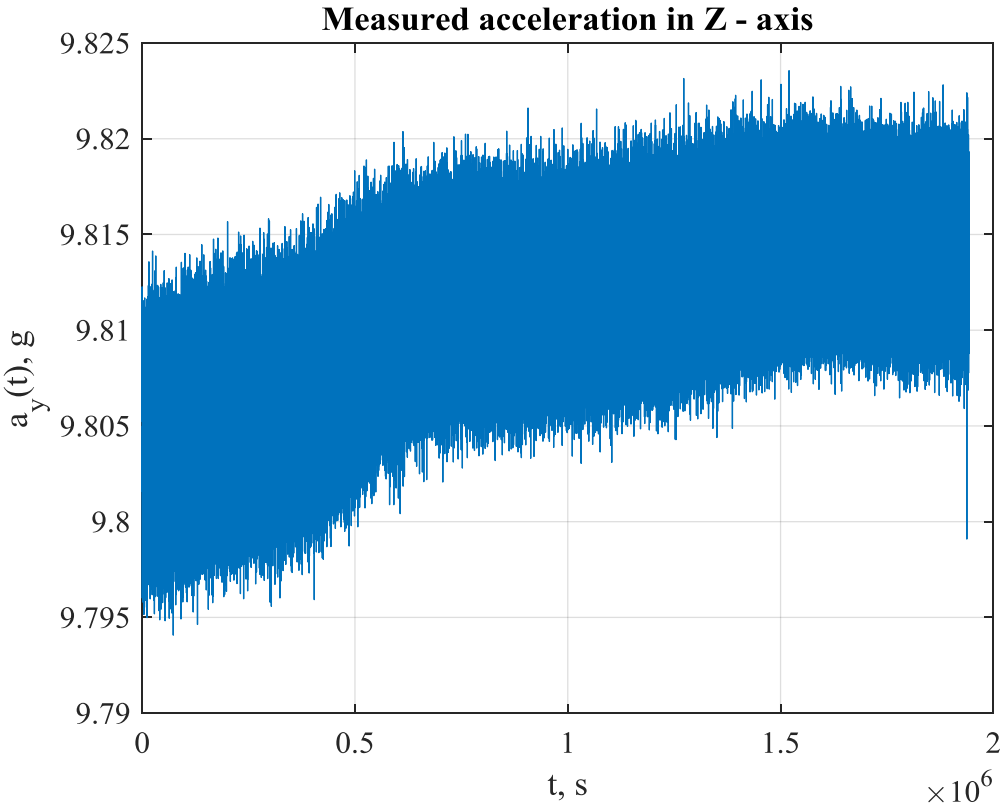

Fig. 3.2.3. Measured acceleration in z-axis

Let us consider the Allan deviation of the Sagem accelerometer in Fig. 3.2.4.

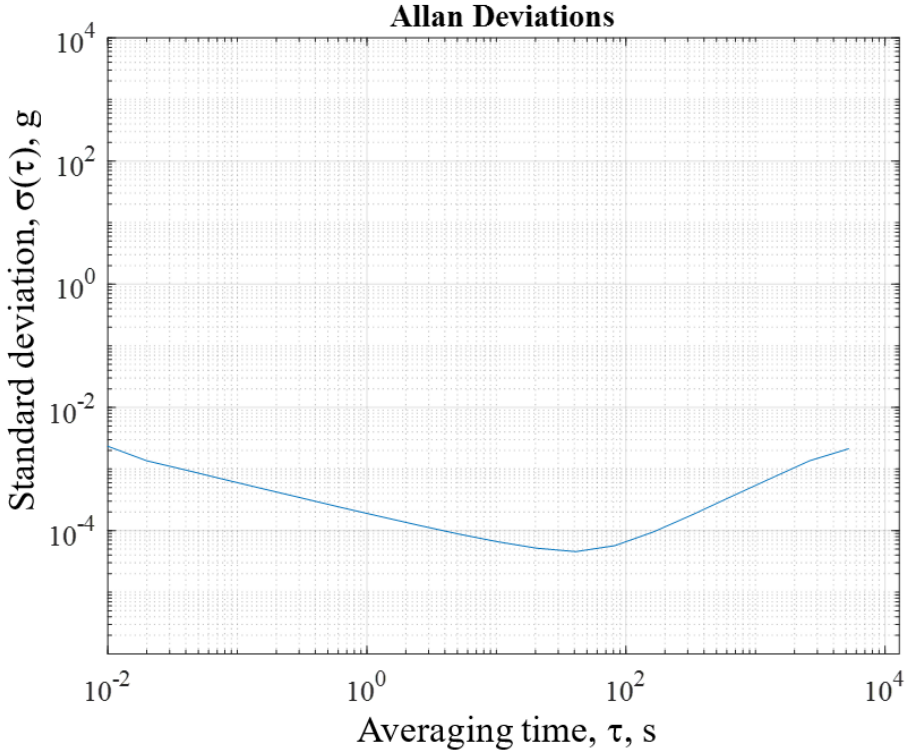

Fig. 3.2.4. Allan standard deviation

The graphs below present an analysis of the three main errors that characterize a Sagem accelerator: velocity random walk, bias instability, and rate random walk. Each graph shows how these errors change over time and under different operating conditions. The results allow us to better understand how these errors affect the accuracy of acceleration measurements under different circumstances.

Fig. 3.2.5 shows the Velocity Random Walk graph, which demonstrates the dependence of the random acceleration error on time. This graph indicates the degree of random variation in the acceleration measurement over time. A low value of Velocity Random Walk indicates that the accelerator is stable in terms of random displacements.

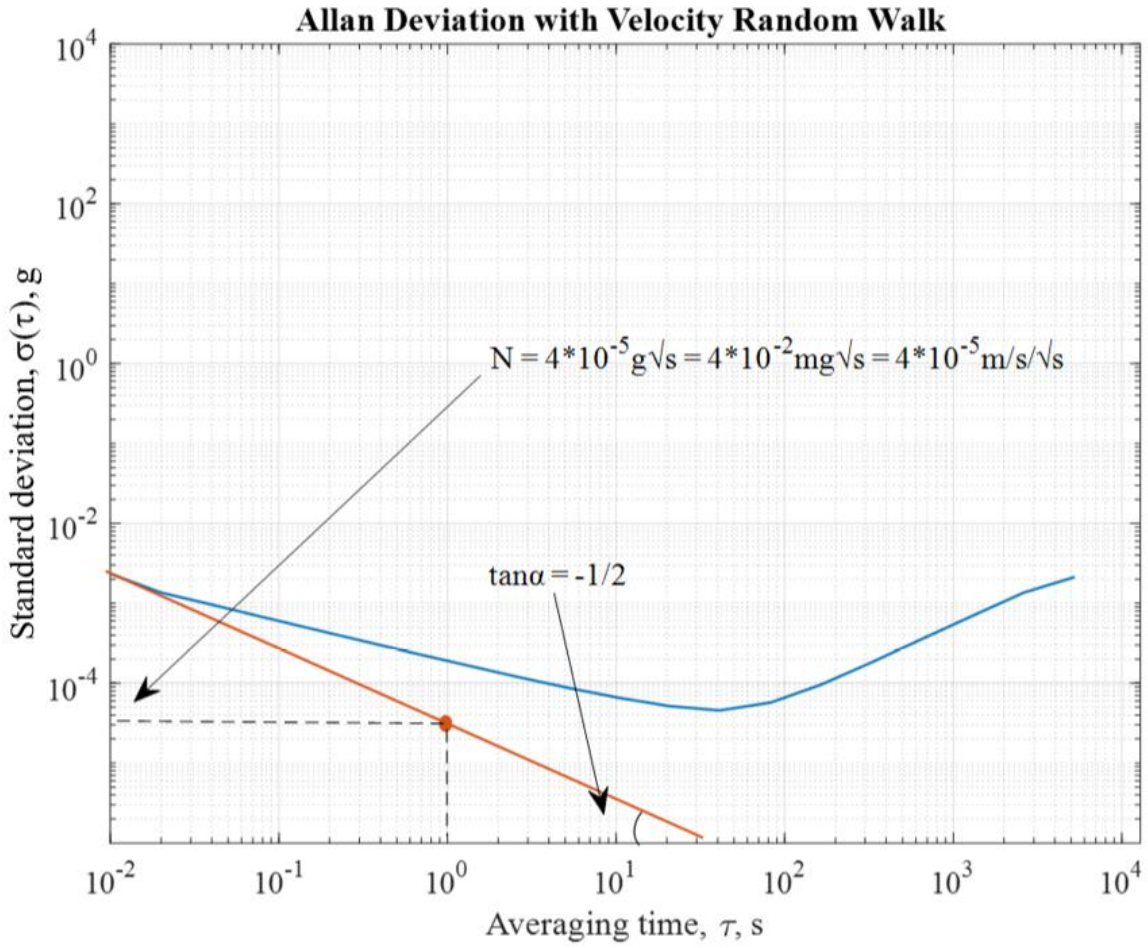

Fig. 3.2.5. Calculation of a velocity random walk

The value of N was determined by finding the point of intersection of the tangent line with a slope of 0.5 and the vertical line starting at time T=1 on the Allan curve.

This point of intersection indicates the value of N, which in this case is

_ _ _

reflecting the noise level or measurement variations in the system.

Fig. 3.2.6 shows the Bias Instability graph, which displays the change in acceleration stability error over time. This graph allows you to assess how much the average value of acceleration measurements changes over time. A low Bias Instability value indicates that the average value of the acceleration measurements does not change much over time, which is important for accurate measurements.

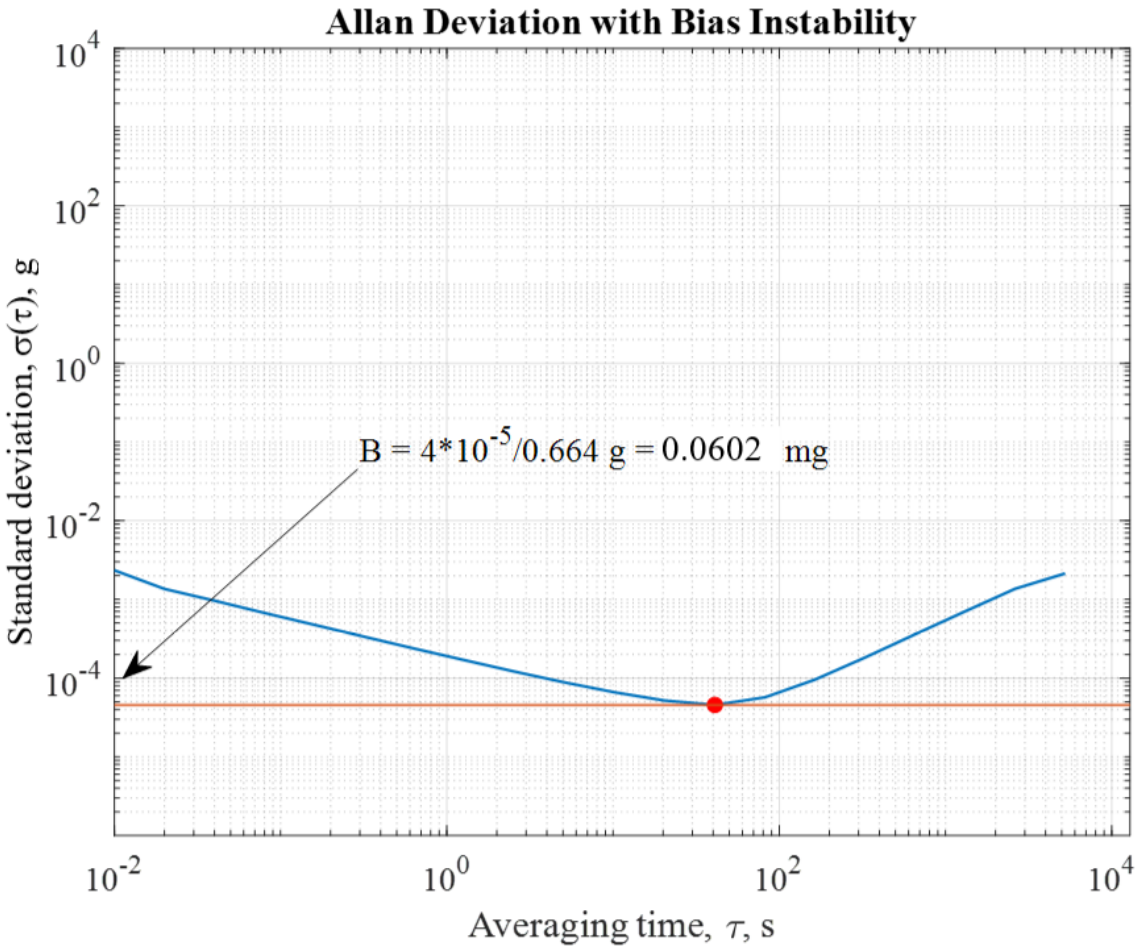

Fig. 3.2.6. Calculation of a bias instability

Finally, Fig. 3.2.7 shows the Rate Random Walk graph, which illustrates the effect of random changes in angular velocity on the accuracy of acceleration measurements. This graph helps determine the stability of the accelerator under random changes in angular velocity.

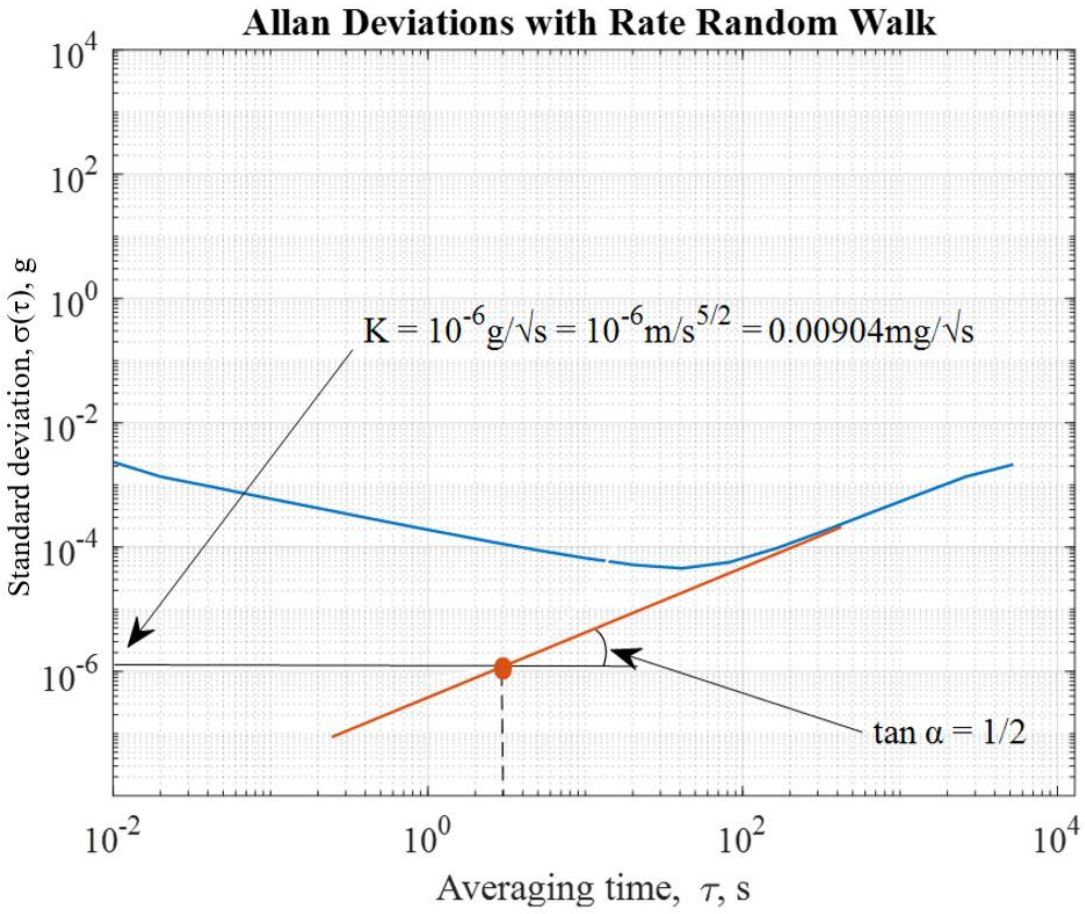

Fig. 3.2.7. Calculation of a rate random walk

The rate random walk is represented by a slope of +0.5 on a log-log plot of $\sigma(\tau)$, and its deviation is given by the formula:

In my example, the value was calculated as follows:

First, was determined to be . Using the given formula, we substitute this value into the equation:

Thus, by following the formula for rate random walk and substituting the appropriate values, we obtain the rate random walk coefficient:

Analyzing these graphs helps to better understand the performance and behavior of the Sagem accelerator during acceleration measurements under various operating conditions [38].

3.3. Interpretation of the results

In this section, we present the following results of calculations related to the effect of temperature on the Sagem accelerometer and its acceleration measurement characteristics. Based on the data collected and calculations performed, we determine the level of stability, accuracy, and reliability of the device under various operating conditions.

We used the Sagem accelerometer to evaluate its performance: Velocity Random Walk (VRW), Bias Instability, and Rate Random Walk (RRW). These indicators allow you to understand what factors affect the accuracy of acceleration measurements and how the device performs under different operating conditions.

Velocity Random Walk (VRW): This indicator indicates the rate of random changes in acceleration measurements over time. In your case, a low value of N = ( ) indicates a low degree of noise in the system, making the Sagem

accelerometer a stable and reliable device for acceleration measurement in applications where high accuracy is important.

Bias Instability: This indicator indicates the change in the average value of acceleration measurements over time. A low Bias Instability value ( ) indicates that the average acceleration value is stable over a long period of time. This is especially important for applications that require accurate acceleration measurement over a long period of time, such as navigation systems or measuring devices.

Rate Random Walk (RRW): This indicator indicates the effect of random changes in angular velocity on the accuracy of acceleration measurements. A low RRW value ( ) indicates that the accelerator is not sensitive to changes in angular velocity. This is important for applications where the object being measured may be subject to various angular motions, such as in aircraft or automotive stabilization systems.

In general, low VRW, Bias Instability, and RRW values indicate high stability and accuracy of Sagem accelerometer acceleration measurements under various operating conditions. This can have a significant impact on various technical applications, including navigation systems, vibration monitoring, and aerospace research, where high accuracy and stability of acceleration measurements are required.

3.4. Conclusion

In this section of the work, calculations were performed using the Allan method to analyze the characteristics of the gyroscope in real-world operation. The calculated parameters, such as Velocity Random Walk (VRW), Bias Instability, and Rate Random Walk (RRW), provided important data on the stability and accuracy of the accelerometer measurements.

Velocity Random Walk indicates the rate of random changes in acceleration measurements over time. A low value of this parameter indicates the stability of the device and its reliability in measuring acceleration.

Bias Instability determines how much the average value of acceleration measurements changes over time. A low Bias Instability value indicates that the average acceleration value is stable, which is important for long-term measurements.

Rate Random Walk indicates the influence of random changes in angular velocity on the accuracy of acceleration measurements. A small value of this parameter indicates a low sensitivity of the accelerometer to changes in acceleration.

Thus, our calculations made it possible to determine the characteristics and behavior of the accelerometer when measuring acceleration under various operating conditions. This is important to ensure accurate and reliable measurements in various technical applications. Further research in this area can help improve the technology and increase the accuracy and reliability of inertial measurement systems.

CONCLUSION

MEMS accelerometers have revolutionized inertial technology, offering compact, cost-effective and high-performance solutions for a wide range of applications in a variety of industries. Their further development and integration into modern IMUs are making a significant contribution to the development of navigation, robotics, automotive safety systems and many other industries that depend on accurate motion measurement and control.

The application of Allan variance analysis to MEMS accelerometers is important in enhancing navigation accuracy by identifying and mitigating noise-related issues that can influence the reliability and precision of navigation systems.

A low value of Velocity Random Walk indicates the rate of random changes in acceleration measurements over time and indicates the stability of the device and its reliability in measuring acceleration.

A low Bias Instability value indicates that the average acceleration value is stable, which is important for long-term measurements.

Rate Random Walk indicates the influence of random changes in angular velocity on the accuracy of acceleration measurements. A small value of this parameter indicates a low sensitivity of the accelerometer to changes in acceleration.

REFERENCES

1. https://www.omega.com/en-us/resources/accelerometers
2. https://support.sbg-systems.com/sc/kb/latest/inertial-measurements-units/accelerometers
3. https://futurenow.com.ua/shho-take-akselerometr-osnovy/
4. https://learn.sparkfun.com/tutorials/accelerometer-basics/all
5. https://www.omega.com/en-us/resources/accelerometers
6. https://en.wikipedia.org/wiki/MEMS
7. https://www.mems-exchange.org/MEMS/what-is.html
8. https://en.wikipedia.org/wiki/MEMS
9. https://support.sbg-systems.com/sc/kb/latest/inertial-measurements-units/accelerometers
10. Аврутов В.В., Бондар П.М., Мелешко В.В. Мікроакселерометри ти їх випробування: Навчальний посібник. 2008 р.
11. П. М. Бондар, Ю. В. Степанковський, Фізичні основи орієнтації і навігації Лабораторний практикум для студентів спеціальності «Прилади і системи орієнтації» – Київ 2011
12. https://www.linkedin.com/pulse/flexible-pendulum-accelerometer-market-research-report-unlocks/
13. https://opticalsolution.lv/products/inertial-measurement-units/
14. Prof Alonzo Kelly, Cambridge University Press 978-1-107-03115-9 – Mobile Robotics: Mathematics, Models, and Methods
15. NMT EE 570: Location and Navigation: Theory & Practice
16. O. Le Traon, D. Janiaud, S. Muller “Monolithic Accelerometer Transducer” US Patent n° 5,962,786 published: 10/05/1999.
17. O. Le Traon, D. Janiaud, M. Pernice, S. Masson, S. Muller and J. -Y. Tridera, "A New Quartz Monolithic Differential Vibrating Beam Accelerometer," 2006

IEEE/ION Position, Location, And Navigation Symposium, Coronado, CA, USA, 2006, pp. 6-15, doi: 10.1109/PLANS.2006.1650581.

18. Kai Daniel Oberlander, Dr. rer. nat. Inverse Kinematics: Joint Considerations and the Maths for Deriving Anatomical Angles. – Sep. 2015
19. http://www.allanstime.com/Publications/DWA/Conversion_from_Allan_variance_to_Spectral_Densities.pdf
20. http://www.allanstime.com/AllanVariance/
21. R. Ramalingam, G. Anitha, J. Shanmugam., Defence Science Journal 59(6):650-658. Microelectromechnical Systems Inertial Measurement Unit Error Modelling and Error Analysis for Low-cost Strapdown Inertial Navigation System – Nov. 2009
22. https://www.everythingrf.com/community/what-is-allan-variance
23. http://www.allanstime.com/Publications/DWA/Conversion_from_Allan_variance_to_Spectral_Densities.pdf
24. Naser El-Sheimy, Haiying Hou, and Xiaoji Niu. Analysis and Modeling of Inertial Sensors Using Allan Variance
25. https://www.allaboutcircuits.com/technical-articles/intro-to-allan-variance-analysis-non-overlapping-and-overlapping-allan-variance/
26. https://www.phidgets.com/docs/Allan_Deviation_Guide#Allan_Variance
27. IEEE Std 952-1997, IEEE Standard Specification Format Guide and Test Procedure for Single Axis Interferometric Fiber Optic, 16 (1997)
28. IEEE Std 962-1997 (R2003) Standard Specification Format Guide and Test Procedure for Single-Axis Interferometric Fiber Optic Gyros, Annex C. IEEE, (2003).
29. Woodman O.J., An introduction to inertial navigation, Cambridge, (2007)
30. Hyunseok Kim, Jang Gyu Lee, Chan Gook Park. Performance Improvement of GPS/INS Integrated System Using Allan Variance Analysis

31. https://www.researchgate.net/publication/356274269_Noise_Analysis_and_Performance_Improvement_of_A_MEMS_Fabry-Perot_Seismic_Accelerometer
32. https://www.researchgate.net/publication/322134773_Measuring_Accelerometer_Dynamic_Range_from_Seismic_Data_Using_Allan_Deviation
33. A.V. Rudyk, Cand.of Tech.Sc, Ass.Prof. National Aviation University – Analysis Of The Errors Of Mems Accelerometers By The Allan Variation Method
34. Liu, X., Wang, J., Liu, F. et al. Spectrum feature extraction method combining Allan variance, VMD, and PSD. Sci Rep 14, 10990 (2024). https://doi.org/10.1038/s41598-024-61176-2
35. Zirkind, Naomi Esther. "Allan Variance Calculation for Nonuniformly Spaced Input Data." (2015).
36. Maddipatla, Satya Prasad, Haeri, Hossein, Jerath, Kshitij, and Brennan, Sean. "Fast Allan Variance (FAVAR) and Dynamic Fast Allan Variance (D-FAVAR) Algorithms for both Regularly and Irregularly Sampled Data". *IFAC-PapersOnLine* 54 (20). https://doi.org/10.1016/j.ifacol.2021.11.148.
37. https://www.allaboutcircuits.com/technical-articles/intro-to-allan-variance-analysis-non-overlapping-and-overlapping-allan-variance/
38. Marinov, Marin & Petrov, Zhivo. ALLAN VARIANCE ANALYSIS ON ERROR CHARACTERS OF LOW-COST MEMS ACCELEROMETER MMA8451Q. 2016